S_N2 Reactivity of CH_3X Derivatives. A Valence Bond Approach

Sason S. Shaik* and Addy Pross

Contribution from the Department of Chemistry, Ben-Gurion University of the Negev, Beer Sheva, 84120 Israel. *Received September 8, 1981*

Abstract: A method for conceptualizing reactivity trends in S_N2 reactions is formulated. The gas-phase S_N2 barrier arises from an avoided crossing of two electronic curves which contain the *reactant-like* and *product-like* Heitler–London VB forms N^-: R· ·X and N· ·R :X^-. The energy separation of the curves at each reaction end is the difference between the ionization energy of the nucleophile ($I_{N:}$) and the electron affinity of the substrate (A_{RX}). The reaction barrier is shown to be a fraction of this energy gap ($I_{N:} - A_{RX}$), and the size of this fraction is shown to depend on the slopes of the intersecting curves. Thus, the height of the barrier is determined by the gap–slope interplay, and it can be represented by one general equation which applies to thermoneutral identity reactions as well as to exothermic nonidentity reactions. These reactivity factors are quantified for a variety of nucleophiles (N^-:) and CH_3X substrates and are used to discuss gas-phase S_N2 barriers for identity and nonidentity reactions. It is suggested that reactivity patterns fall into two categories: (a) *electron-transfer-controlled* patterns which are dominated by the size of energy gap $I_{N:} - A_{CH_3X}$ (these trends are found whenever N and X are varied down a column of the periodic table); and (b) *slope-controlled* patterns in which reactivity is determined by the strength of the $(C.\therefore X)^-$ and $(C.\therefore N)^-$ 3-electron bonds. Whenever these bonds are strong, reactivity is reduced. Increasing the number of possible leaving groups, e.g., as in CH_4, CH_2Cl_2, CCl_4, has a similar slope effect leading to low reactivity. The effect of ΔH is investigated. It is shown that whenever the gap factor and the slope factors operate in opposition, increasing the reaction exothermicity does not guarantee increasing reactivity. Thus, the dominant role of slope factors is suggested to be the root cause in the occasional breakdown of the Bell–Evans–Polanyi principle.

What is the electronic origin of the barrier for S_N2 reactions in the gas phase[1,2] and in solution?[3] What properties make a certain reactant pair of nucleophile and substrate react faster than another? It is evident that in order to conceptualize such reactivity trends one must first answer the fundamental question: *how does the barrier arise*? Once a way of describing barrier formation is found, this may provide a means of comprehending the effect of substitutents and solvents on the barrier height.

In previous papers[4] we have shown that the S_N2 profile is generated by an avoided crossing[5] of two electronic curves and we have illustrated how one can conceptualize the transition state in terms of the makeup of the intersection point.[4b,6-8] In the present paper we shall develop this idea further and use the avoided crossing model to analyze thermoneutral as well as exothermic gas-phase S_N2 reactions. The S_N2 barrier will be shown to depend on two factors which are direct offsprings of the model: (a) the initial energy gap of the two intersecting curves, which is related to the *donor–acceptor relationship* between the reactants and (b) the slopes of the intersecting curves which are related to various *localization requirements* of the reactants and to the eaction exothermicity.

These reactivity variables will be quantified and used as predictors of reactivity trends in the S_N2 reaction of CH_3X systems.

I. Theory

Let us consider the S_N2 reaction of a nucleophile (N^-:) which acts as an electron donor (D) with a substrate (R–X) which reacts as an electron acceptor (A).

$$\underset{D}{N^-:} + \underset{A}{R-X} \rightarrow N-R + :X^- \qquad (1)$$

The bond reorganization associated with the reaction primarily involves the four reacting electrons which are reshuffled during the transformation.[9] These are the lone-pair electrons of N^-: and

(1) Much of the elegant gas-phase mechanistic work appears in (a) Bohme, D. K.; Young, L. B. *J. Am. Chem. Soc.* **1970**, *92*, 7354–7358. (b) Bohme, D. K.; Mackay, G. I.; Payzant, J. D. *Ibid.* **1974**, *96*, 4027–4028. (c) Lieder, C. A.; Brauman, J. I. *Ibid.* **1974**, *96*, 4029–4030. (d) Brauman, J. I.; Olmstead, W. N.; Lieder, C. A. *Ibid.* **1974**, *96*, 4030–4031. (e) Tanaka, K.; Mackay, G. I.; Payzant, J. D.; Bohme, D. K. *Can. J. Chem.* **1976**, *54*, 1643–1659. (f) Olmstead, W. N.; Brauman, J. I. *J. Am. Chem. Soc.* **1977**, *99*, 4019–4028. (g) Pellerite, M. J.; Brauman, J. I. *Ibid.* **1980**, *102*, 5993–5999. (h) Bohme, D. K.; Mackay, G. I. *Ibid.* **1981**, *103*, 978–979. (i) Smith, M. A.; Barkley, R. M.; Ellison, G. B. *Ibid.* **1980**, *102*, 6851–6852. (j) For unusual leaving groups, see: De Puy, C. H.; Bierbaum, V. M.; Flippin, L. A.; Grabowski, J. J.; King, G. K.; Schmitt, R. J.; Sullivan, S. A. *Ibid.* **1980**, *102*, 5012–5015. (k) For a general account, see: Bowie, J. H. *Acc. Chem. Res.* **1980**, *13*, 76–82.

(2) Ab initio computations also indicate the existence of a central barrier in S_N2 reactions. (a) Dedieu, A.; Veillard, A. *J. Am. Chem. Soc.* **1972**, *94*, 6730–6738. (b) Dedieu, A.; Veillard, A. *Chem. Phys. Lett.* **1970**, *5*, 328–330. (c) Duke, A. J.; Bader, R. F. W. *Ibid.* **1971**, *10*, 631–635. (d) Bader, R. F. W.; Duke, A. J.; Messer, R. R. *J. Am. Chem. Soc.* **1973**, *95*, 7715–7721. (e) Ishida, K.; Morokuma, K.; Komornicki, A. *J. Chem. Phys.* **1977**, *66*, 2153–2156. (f) Keil, F.; Ahlrichs, R. *J. Am. Chem. Soc.* **1976**, *98*, 4787–4793. (g) Baybutt, P. *Mol. Phys.* **1975**, *29*, 389–403. (h) Dyczmons, V.; Kutzelnigg, W. *Theor. Chim. Acta* **1974**, *33*, 239. (i) Van der Lugt, W. Th. A.M.; Ros, P. *Chem. Phys. Lett.* **1969**, *4*, 389. (j) Ritchie, C. D.; Chappell, G. A. *J. Am. Chem. Soc.* **1979**, *92*, 1819. (k) Mulder, J. J. C.; Wright, J. S. *Chem. Phys. Lett.* **1970**, *5*, 445. (l) Berthier, G.; David, D.-J.; Veillard, A. *Theor. Chim. Acta* **1969**, *14*, 329. (m) Wolfe, S.; Mitchell, D. J. *J. Am. Chem. Soc.* **1981**, *103*, 7693. (n) Wolfe, S.; Mitchell, D. J.; Schlegel, H. B. *Ibid.* **1981**, *103*, 7694.

(3) Recent discussions of the S_N2 mechanism in solution and the possible sources of its barrier [(a) using Marcus theory and (b) the BEBO approach], along with extensive lists of computed and experimental barriers, are as follows: (a) Albery, W. J.; Kreevoy, M. M. *Adv. Phys. Org. Chem.* **1978**, *16*, 85–157. (b) McLennan, D. J. *Aust. J. Chem.* **1978**, *31*, 1897–1909.

(4) (a) Shaik, S. S. *J. Am. Chem. Soc.* **1981**, *103*, 3692–3701. (b) Pross, A.; Shaik, S. S. *Ibid.* **1981**, *103*, 3702–3709. (c) Shaik, S. S. Nouv. *J. Chim.*, in press.

(5) A lucid discussion of avoided crossing is given in: Salem, L.; LeForestier, C.; Segal, G.; Wetmore, R. *J. Am. Chem. Soc.* **1975**, *97*, 479–487.

(6) Other theories which predict the structure of the transition state are those of: (a) Thornton, E. R. *J. Am. Chem. Soc.* **1967**, *89*, 2915. (b) More O'Ferrall, R. A. *J. Chem. Soc. B* **1970**, 274. (c) Harris, J. C.; Kurz, J. L. *J. Am. Chem. Soc.* **1970**, *92*, 349. (d) Critchlow, J. E. *J. Chem. Soc., Faraday Trans.* **1972**, *68*, 1774. (e) Jencks, D. A.; Jencks, W. P. *J. Am. Chem. Soc.* **1977**, *99*, 7948. (f) McLennan, D. J. *J. Chem. Soc., Faraday Trans. 1* **1975**, 1516–1527.

(7) For recent reviews on the structure of the transition state, see: (a) More O'Ferrall, R. A. In "The Chemistry of the Carbon Halogen Bond"; Patai, S., Ed.; Wiley: New York, 1973; Vol. 2, p 609. (b) Jencks, W. P. *Chem. Rev.* **1972**, *72*, 705. (c) Kresge, A. J. *Acc. Chem. Res.* **1975**, *8*, 354. (d) Westheimer, F. H. *Chem. Rev.* **1961**, *61*, 265. (e) Albery, W. J. *Prog. React. Kinet.* **1967**, *4*, 355. (f) Bruice, T.C. *Annu. Rev. Biochem.* **1976**, *45*, 331. (g) Pross, A. *Adv. Phys. Org. Chem.* **1977**, *14*, 69. (h) McLennan, D. J. *Tetrahedron* **1975**, *31*, 2999. (i) Johnson, C. D. *Chem. Rev.* **1975**, *75*, 755.

(8) Many of the ideas associated with the above theories[6] are related to Hammond's postulate and Leffler's relationship which are based on the Brønsted equation and the Bell–Evans–Polanyi relationship (BEP). (a) Hammond, G. S. *J. Am. Chem. Soc.* **1955**, *77*, 334. (b) Leffler, J. E. *Science (Washington, D.C)* **1953**, *117*, 340. (c) Leffler, J. E.; Grunwald, E. "Rates and Equilibria in Organic Chemistry"; Wiley: New York, 1963. (d) Brønsted, J. N.; Pedersen, K. J. *Z. Phys. Chem. (Leipzig)* **1924**, *108*, 185. (e) Bell, R. P. *Proc. R. Soc. London, Ser. A* **1936**, *154*, 414. (f) Evans, M. G.; Polanyi, M. *Trans. Faraday Soc.* **1936**, *32*, 1340.

0002-7863/82/1504-2708$01.25/0

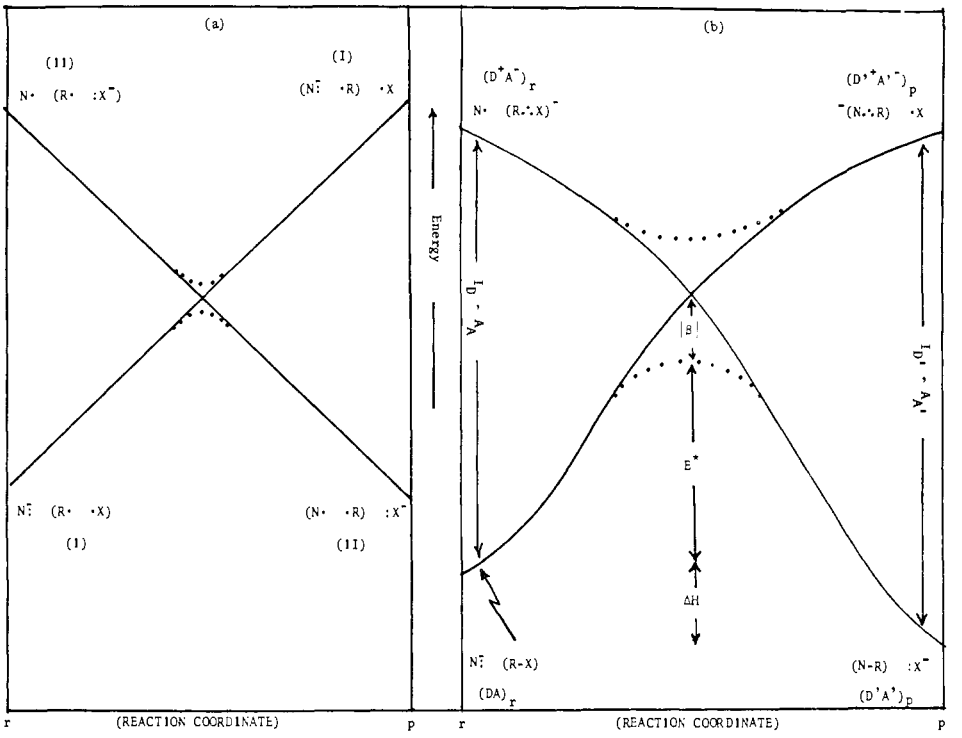

Figure 1. (a) Avoided crossing (dotted lines) of the reactant-like and product-like Heitler–London VB forms (I and II) for an S_N2 reaction. (b) State correlation diagram after inclusion of VB configurations III and IV. $(R.\therefore X)^-$ and $(N.\therefore R)^-$ represent 3-electron bonds while R–X and N–R represent 2-electron bonds. The intended correlations are $(DA)_r \rightarrow (D'^+A'^-)_p$ and $(D^+A^-)_r \rightarrow (D'A')_p$ where the nucleophiles (N^-:, X^-:) are the donors (D, D') and the substrates (R–X, N–R) are the acceptors (A, A'). $I_D - A_A$ and $I_{D'} - A_{A'}$ are the energy gaps at the reaction ends. $|\beta|$ is the degree of avoided crossing and E^* is the barrier for the forward reaction. ΔH is the reaction exothermicity. Diagrams are schematic.

the bond-pair electrons of R–X. In previous papers[4a,b] we have shown that *this electronic reshuffle takes the form of an avoided crossing*[5] *between two electronic curves, thereby leading to formation of a barrier.* This avoided crossing is latent in the delocalized MO picture and does not readily reveal the electronic origins of the barrier. However, by expanding the delocalized MO wave functions into the component VB building blocks, one finds[4a] that this avoided crossing is nothing else but an interchange of two Heitler–London[10] VB bond forms whose switchover reflects the bond interchange and the electron jump ($N: \rightarrow RX$). This was a key conclusion in our previous papers.[4]

Let us go back now and develop these ideas briefly. The two Heitler–London VB forms which correspond to reactants and products are shown below in I and II, respectively.[4a,b]

$$\underset{\text{I}}{N^-:R\cdot\cdot X} \qquad \underset{\text{II}}{N\cdot\cdot R:X^-}$$

R· ·X and N· ·R are spin-paired forms which constitute the covalent components of the R–X and the N–R bonds, respectively, and can be represented pictorially in terms of a resonance interaction between two spin-exchanged structures, i.e.[11a]

$$R\cdot\cdot X \equiv 2^{-1/2}\{R^{\cdot\uparrow}\,{}^{\downarrow}\cdot X \leftrightarrow R^{\cdot\downarrow}\,{}^{\uparrow}\cdot X\} \qquad (2)$$

In order to illustrate the avoided crossing of these two forms I and II, we have to consider the variations in their energies along the S_N2 reaction coordinate.[4c] This is shown in Figure 1a. Initially when the N– –R distance is large and the R– –X distance is small, the most stable form is the reactant-like form (I) which enjoys 2-electron stabilization across the RX linkage.[11b] At the same geometry the second VB structure (II) is an *excited form* of I, and the two forms differ by a *single electron transfer* from N^-: to the RX moiety. This second moiety is destabilized by the unfavorable 3-electron interaction in R· $:X^-$.[12]

As we proceed along the reaction coordinate from reactants (r) to products (p), the energy of form I goes up since the favorable R· ·X 2-electron interaction is gradually broken and replaced by a destabilizing N^-: ·R 3-electron interaction.[4b,12] Form II behaves in exactly the opposite manner; its energy goes down along the reaction coordinate since a stabilizing N· ·R 2-electron interaction is formed and, at the same time, the destabilizing R· $:X^-$ 3-electron interaction is reduced. At some point, an energy equality, $E(I) = E(II)$, is achieved, and eventually, as the full potential of the N· ·R interaction is realized and the R· $:X^-$ interaction is released, the two forms cross, and II becomes the most stable form at the product end (p). The avoided crossing (or interaction[13]) of the two forms at the intersection point leads to the formation of a barrier on the lower energy curve, as shown in Figure 1a. This is the source of the S_N2 barrier which will persist even after the inclusion of other VB forms and solvation terms.[14]

We must now refine our picture, since certainly there are additional contributors to the wave function other than just forms I and II. The foremost important VB structures among those

(9) See ref 4a. The same conclusions was expressed many times before by Fukui. See, for example: Fukui, K. "Theory of Orientation and Stereoselection"; Springer Verlag: Heidelberg, 1975.

(10) Heitler, W.; London, F. *Z. Phys.* **1927**, *44*, 455.

(11) (a) Overlap is neglected in the normalization constant. (b) The resonance or, as it is often called, the exchange stabilization is due to the term, $2\beta_{RX}S_{RX}$ (β-resonance integral) and is taken to be the covalent portion of the R–X bond energy (H^0_{R-X}). It is approximated by the Pauling relation $\sim -(H^0_{R-R}H^0_{X-X})^{1/2}$. See: Pauling, L.; Wilson, E. B., Jr. "Introduction to Quantum Mechanics"; McGraw Hill: New York, 1935. Pauling, L. "The Nature of the Chemical Bond"; Cornell University Press: Ithaca, NY, 1960. Slater, J. C. "Quantum Theory of Molecules and Solids"; McGraw-Hill: New York, 1963; Vol. 1.

(12) The 3-electron destabilization in the localized form R· $:X^-$ is due to the term $-2\beta_{RX}S_{RX}$ in the energy expression. Thus, there is actually 3-electron overlap repulsion in its VB formulation. For discussions, see Pauling and Wilson,[11b] pp 326–366. Coulson, C. A. "Valence"; Oxford University Press: London, 1961; pp 147, 158–161. The explicit energy expressions are available in: Shaik, S. S. Ph.D. Thesis, Seattle, Washington, 1978.

(13) The interaction $\langle N:^- R\cdot\cdot X|\hat{H}|N\cdot R\cdot :X^-\rangle$ is proportional to the overlap of N and X (i.e., quite small) and leads to splitting of the intersection point into two states which are $2^{-1/2}$ (I ± II).

(14) This description is similar to the Evans–Polanyi treatment and to a recent treatment by Warshel. (a) Evans, M. G.; Polanyi, M. *Trans. Faraday Soc.* **1938**, *34*, 11. (b) Ogg, R. A., Jr.; Polanyi, M. *Ibid.* **1935**, *31*, 604. (c) Warhurst, E. *Q. Rev.* (*London*) **1951**, *5*, 44. (d) See also: Laidler, K.; Shuler, K. E. *Chem. Rev.* **1951**, *48*, 153–224. (e) Warshel, A.; Weiss, R. M. *J. Am. Chem. Soc.* **1980**, *102*, 6218–6226.

remaining are the carbenium configuration, III, and the carbanion configuration, IV.

$$\underset{\text{III}}{N^-: R^+ :X^-} \qquad \underset{\text{IV}}{N\cdot\ R^-: \cdot X}$$

Two configurations interact proportionally to the resonance integral, β, of the atomic sites which differ by one electron occupancy in the two configurations.[4,15] At the reactant end (r), the only possible mixing is that which is caused by interactions across the RX linkage. Therefore, as we "turn on" the VB mixing, form III will interact only with form I via the β_{RX} atomic resonance integral,[15] thereby providing the covalent R–X 2-electron bond with its polar character and its full bonding potential:[16]

$$N^-: \{a(R\cdot\ \cdot X) \leftrightarrow b(R^+ :X^-)\} \equiv N^-: (R\text{–}X) \qquad (a > b) \quad (3)$$

At the same geometry, form IV can interact only with the excited form II but not with the ground form I. This interaction which is again of a β_{RX} type resonance integral, though of different magnitude, causes some delocalization of the three electrons in the RX moiety and leads to the so-called 3-electron bond.[4b,17] This is described in reaction 4 by the symbolic delocalized form $(R\therefore X)^-$.[18]

$$N\cdot\ \{a(R\cdot\ :X^-) \leftrightarrow b(R^-: \cdot X)\} \equiv N\cdot\ (R\therefore X)^- \qquad (a > b) \quad (4)$$

One must be careful though to remember that this 3-electron bond is not in its most stable configuration since it has the same R– –X contact as in the neutral substrate.

At the product end (p) of the reaction, the R– –X distance is large while the N– –R distance is small, and therefore forms III and IV reverse their mixing pattern with I and II. The carbenium form III can now only interact with the ground-form II via the β_{NR} resonance integral, thereby providing the N–R bond with some polar character and its full bonding potential:[16]

$$\{a(N\cdot\ \cdot R) \leftrightarrow b(N^-: R^+)\}X^- \equiv (N\text{–}R)\ X^-: \qquad (a > b) \quad (5)$$

The carbanion configuration on the other hand, can only interact with the excited form I via β_{NR}', leading to the $(N\therefore R)^-$ 3-electron bond (whose N– –R contact equals that in the product N–R).[18]

$$\{a(N^-: \cdot R) \leftrightarrow b(N\cdot\ :R^-)\}X\cdot \equiv (N\therefore R)^-\ X\cdot \qquad (a > b) \quad (6)$$

We have now generated (eq 3–6) the corrected ground and excited forms at the two reaction ends, and they are shown in Figure 1b. In so doing, we have defined and characterized four *anchor points* for the two intersecting curves. This characterization is of prime importance and will be the basis for many of our future arguments. Figure 1b shows a pairwise intended correlation of these four forms. A ground form at one end intends to correlate with an excited form at the other end and vice versa, i.e., $N^-: (R\text{–}X) \rightarrow (N\therefore R)^- \cdot X$ and $N\cdot(R\therefore X)^- \rightarrow (N\text{–}R) :X^-$. Through the mixing of the forms the intended correlation is avoided, and two new curves are generated, with the lower one having a barrier (E^*) whose top is the transition state for the thermal reaction.[19] Clearly, Figure 1b is a form of a state *correlation diagram*[20] in which the intended correlation is dictated by the electronic redistribution brought about by the interchange of the reactant-like and product-like Heitler–London bond forms of Figure 1a (I and II).

This discussion applies to substrates and nucleophiles which are bona fide S_N2 systems, such as CH_3X, where VB forms III and IV are always subsidary forms compared to I and II. However, there are systems such as for R = $ArCR'_2$–, NC–CR'_2–, etc., where either III or IV are substantially stabilized and can sometimes become lower in energy than the intersection point of forms I and II (Figure 1a). Consequently they can lead either to borderline mechanisms (e.g., S_N1–S_N2)[4b] or to formation of intermediates (e.g., carbonium ion species in the case of III) along the reaction coordinate. Our discussion does not cover these cases and will be limited to the bona fide S_N2 substrates CH_3X.[21]

At this stage we have a description of barrier formation in the S_N2 reaction. Before we seek out the elements which affect the height of this barrier, we must use more familiar terminology in order to lend our model additional insight and predictive value. Thus, we refer back to the definitions we used in eq 1, where we assigned the nucleophile (N^-:) the role of electron donor (D) and the substrate (R–X) the role of electron acceptor (A). Using this terminology, the ground form, $N^-: (R\text{–}X)$, at the reactant end (r) in Figure 1b is equated with the no-bond valence state, $(DA)_r$, while the exicted form, $N\cdot(R\therefore X)^-$, which is related to $(DA)_r$ by *a single electron transfer* ($N \rightarrow RX$), is the charge-transfer valence state,[22] $(D^+A^-)_r$. In the case of the reverse reaction the donor is now X^-: while the acceptor is N–R, and hence, the two anchor points (Figure 1b) are the products no-bond $(D'A')_p$ and charge-transfer $(D'^+A'^-)_p$ valence states. This is indicated in Figure 1b which illustrates that the no-bond state of the reactants intends correlating with the charge-transfer state of the product i.e., $(DA)_r \rightarrow (D'^+A'^-)_p$ and vice versa $(D^+A^-)_r \rightarrow (D'A')_p$. This means that both in the forward and in the reverse reactions, the S_N2 profile can be described in terms of a DA – D^+A^- intersection.[23] Initially, at some D···A encounter distance, the energy

(15) Rules for taking matrix elements between Slater determinants are given inter alia in: McGlynn, S. P.; Vanquickenborne, L. G.; Kinoshita, M.; Carroll, D. G. "Introduction to Applied Quantum Chemistry"; Holt, Rinehart and Winston: New York, 1972; pp 281–298. The matrix elements are with respect to an effective one-electron Hamiltonian.

(16) We consistently neglect the contribution of the $R^-: X^+$ form to bonding. Therefore the configurations $N^+ R^-$; X^-: and $N^-: R^-$: X^+ are not included in the discussion. While for a proper description of bonding, both are needed, their importance is marginal for most qualitative purposes. See 14e also.

(17) For discussions on the 3-electron bond, see, for example, (a) Pauling Wilson,[11b] pp 326–366. (b) Goddard, W. A., III; Dunning, T. H., Jr.; Hunt, W. J.; Hay, P. J. *Acc. Chem. Res.* **1973**, *6*, 368–376. (c) Wang, J. T.; Williams, F. *J. Am. Chem. Soc.* **1980**, *102*, 2860–2861. (d) Martin, J. C. "Organic Free Radicals"; Pryor, W. A., Ed.; American Chemical Society: Washington, DC, 1978; ACS Symp. Ser. No. 69, pp 71–88. (e) Perkins, C. W.; Martin, J. C.; Arduengo, A. J.; Lau, W.; Alegria, A.; Kochi, J. K. *J. Am. Chem. Soc.* **1980**, *102*, 7753–7759. (f) Harcourt, R. D. *Ibid.* **1978**, *100*, 8060–8062; **1980**, *102*, 5195–5201. (g) Griller, D.; Lossing, F. P. *Ibid.* **1981**, *103*, 1586–1587. (h) Musker, K. W. *Acc. Chem. Res.* **1980**, *13*, 200–206. (i) Asmus, K.-D. *Acc. Chem. Res.* **1979**, *12*, 436–442.

(18) This symbolism $(R\therefore X)^-$ is used by Bunnett and was adopted by us. Bunnett has devoted considerable effort to study the $S_{RN}1$ mechanism in which a π-type anion radical undergoes cleavage through a σ-type 3-electron bonded $(R\therefore X)^-$ species. See, for example: (a) Bunnett, J. F. *Acc. Chem. Res.* **1978**, *11*, 413–420. (b) Rossi, R. A.; Bunnett, J. F. *J. Org. Chem.* **1973**, *38*, 3020–3025. (c) Bunnett, J. F.; Creary, X. *Ibid.* **1975**, *40*, 3740–3743. (d) Bunnett, J. F.; Creary, X.; Sundberg, J. E. *Ibid.* **1976**, *41*, 1707–1709. (e) Rossi, R. A.; Bunnett, J. F. *Ibid.* **1973**, *38*, 3020–3025. (f) Bunnett, J. F.; Creary, X. *Ibid.* **1974**, *39*, 3173–3174, 3611–3613. (g) Bard, R. R.; Bunnett, J. F.; Creary, X.; Tremelling, M. J. *J. Am. Chem. Soc.* **1980**, *102*, 2852–2854.

(19) (a) This transition state arises from the mixing of III and IV into $\psi_i = 2^{-1/2}(I + II)$. Now the avoided crossing is larger than in Figure 1a. (b) The molecular orbital analogue of this description is discussed in ref 4a in terms of a CI-corrected 4 electron-3 molecular orbital system.

(20) Similar correlation diagrams for photochemical reactions were discussed in terms of the natural correlations of MOs by: (a) Devaquet, A.; Sevin, A.; Bigot, B. *J. Am. Chem. Soc.* **1978**, *99*, 946–948. (b) Bigot, B.; Devaquet, A.; Turro, N. J. *J. Am. Chem. Soc.* **1981**, *103*, 6–12.

(21) The minor role of the carbenium configuration (even in solution reactions of CH_3X) can be deduced from: (a) McLennan, D. J. *Acc. Chem. Res.* **1976**, *9*, 281–287. (b) Abraham, M. H. *J. Chem. Soc., Perkin Trans. 2* **1973**, 1893–1899. (c) Abraham, M. H.; McLennan, D. J. *Ibid.* **1977**, 873–879.

(22) We use the term valence to distinguish our A^- from one having the extra electron in a diffused orbital on carbon. Our A^- accommodates the extra electron in the valence orbitals computed for the neutral species. See, for example, the valence segment for CH_3Cl^- in: Canadell, E.; Karafiloglu, P.; Salem, L. *J. Am. Chem. Soc.* **1980**, *102*, 855–857.

(23) (a) A DA–D^+A^- intersection in S_N2 using MO configurations was first described in: Mulliken, R. S.; Person, W. B. "Molecular Complexes"; Wiley-Interscience: New York, 1969. See also: Epiotis, N. D. *Pure Appl. Chem.* **1979**, *51*, 203–231. For aromatic substitutions, see: Nagakura, S. *Tetrahedron Suppl. 2* **1963**, *19*, 361–377. Epiotis, N. D.; Shaik, S. *J. Am. Chem. Soc.* **1978**, *100*, 29–33. (b) The valence state DA in the present treatment is a linear combination of the MO configurations $\phi_N^2\sigma^2$, $\phi_N^2\sigma^1\sigma^{*1}$, and $\phi_N^2\sigma^{*2}$. The latter two clean some of the ionicity of the C–X bond which is exaggerated in $\phi_N^2\sigma^2$. Similarly our D^+A^-, here, is a linear combination of the configurations $\phi_N^1\sigma^2\sigma^{*1}$ and $\phi_N^1\sigma^1\sigma^{*2}$ which lead to the description of the $(R\therefore X)^-$ bond (eq 4). The MO configurations $\phi_N^2\sigma^2$ and $\phi_N^1\sigma^2\sigma^{*1}$ are approximations to our DA and D^+A^-. See footnote 19 in ref 4b, and discussion in 4a, for the relations of the MO configurations to these valence states.

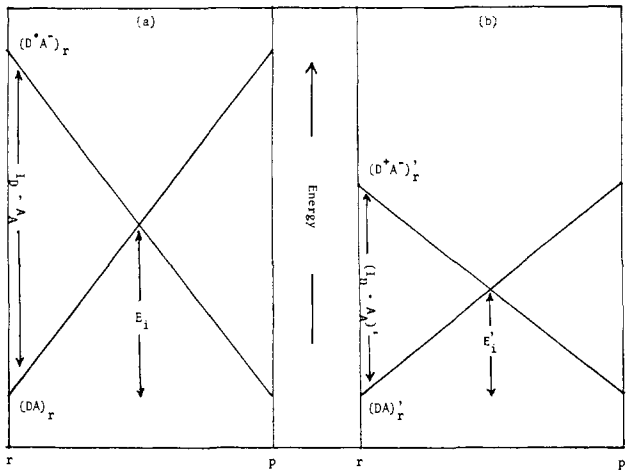

Figure 2. Schematic description of the effect of the donor–acceptor abilitites of the reactants ($I_D - A_A$) on the energy of the intersection point. The initial gap ($I_D - A_A$) in (a) is larger than in (b), and hence $E_i > E_i'$.

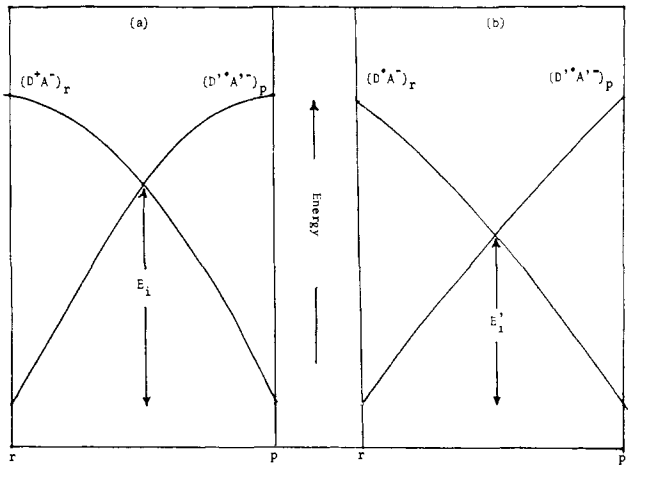

Figure 3. Schematic description of the effect of the slopes of the D^+A^- curves (prior to their intersection) on the energy of the intersection point. The slope in (a) is smaller than in (b), and hence $E_i > E_1'$.

gap between the two curves is given by the difference between the ionization potential of the donor (I_D) and the valence electron affinity of the acceptor (A_A), which in the case of the forward reaction becomes[24]

$$E(D^+A^-) - E(DA) = I_D - A_A \equiv I_{N:} - A_{CH_3X} \qquad (7)$$

Then, as bond reorganization gradually takes place, the two curves cross over. It is quite clear therefore that we can describe the S_N2 reaction as *a transformation which involves a single electron transfer ($D \rightarrow A$) taking place synchronously with bond reorganization.*[25]

In the following sections we use our model to suggest factors which are related to these two aspects and which determine the height of the S_N2 barrier. Our present treatment will be limited to gas-phase reactions of CH_3X, and its major part will be directed toward understanding trends in the height of the "intrinsic" barrier of identity reactions where $N^-: = X^-:$ (eq 1). Less space will be devoted to nonidentity reactions ($N^-: \neq X^-:$ in eq 1) where we shall focus on the role of the thermodynamic driving force.

II. Reactivity Factors in S_N2 Reactions

The picture which emerges from the previous discussion and from Figure 1b is of two intersecting curves which are anchored at four points. At each reaction end the energy gap between the two curves is given by the difference between the ionization potential of the donor and the electron affinity of the acceptor, i.e., $I_{N:} - A_{CH_3X}$ at the reactant end and $I_{X:} - A_{CH_3N}$ at the product end (Figure 1b), while the energy difference between the two ground anchor points is given by the reaction enthalpy, ΔH.[26] The reaction barrier for either the forward or the reverse reaction will always be some fraction of the initial energy gap between the two intersecting curves. Hence, variations in the barrier's height will be dominated by the size of this initial gap and by the relative slopes of the two curves, which for a given gap determine the height of the intersection point, and thereby the fraction of this gap which enters the activation process. Thus we now have at hand two barrier-controlling factors which are direct offsprings of the model: *initial gap* and *slopes* of the two intersecting curves.

The first and the most obvious factor is the initial $(DA)_r - (D^+A^-)_r$ energy gap, $I_D - A_A$ (eq 7, Figure 1b). As the donor and the acceptor abilities of the reactants are improved, the initial energy gap becomes smaller, and as a result the intersection point will move to lower energy. This is a simple outcome of the mutual translation of the two curves as shown schematically in Figure 2. Thus, we can formulate *the first reactivity rule: all other factors being equal, as the reactant pair* $N:, CH_3X$ *becomes a better donor–acceptor pair, the reaction barrier will become smaller.*

As to the slope factor, it is, in principle, possible that two reaction systems which have the same $I_D - A_A$ initial gap may nevertheless exhibit completely different reactivitites owing to different energy variations of the two intersecting curves along the S_N2 reaction coordinate. There are many factors which combine to determine the slopes of the curves, e.g., bond making, bond breaking, angular variations, nonbonded interactions of various sorts, etc., and it is therefore a formidable task to try and *qualitatively* consider how each such factor varies within a large set of reactions. What we *can* hope for, however, is to isolate a few key factors which may be dominant ones and thereby attempt to formulate a theory which does not merely rationalize but also makes verifiable predictions.[27]

Let us first consider the intersection point as arising from the meeting of the *two descending curves* which start out as $(D^+A-)_r$ and $(D'^+A'^-)_p$. Figure 3 describes schematically two possible cases. In Figure 3a the two curves descend slowly in the region prior to their intersection point and thereby generate a high energy intersection point (E_i) which constitutes a large fraction of the initial $I_D - A_A$ energy gap. In contrast when the two curves descend rapidly in the same region they generate a low energy intersection point (E_i') which involves a smaller fraction of the initial energy gap. Thus, we can formulate *a second reactivity rule: for a given donor–acceptor ability (and reaction enthalpy), the* S_N2 *reaction barrier increases as the slopes of the curves* $(D^+A^-)_r$ *and* $(D'^+A'^-)_p$ *decrease in the region before their intended crossing point.*

The descent of D^+A^- from its initial high energy point involves two effects: the first is the localization and breakup of the 3-electron bond in A^- (eq 4 and 6), and the second is the generation

(24) This is an approximation since the DA encounter complex enjoys ion–dipole stabilization (~10 kcal/mol) in the gas phase. See: Dougherty, R. C.; Roberts, J. D. *J. Org. Mass. Spectrom.* **1974**, *8*, 81. Dougherty, R. C. *Ibid.* **1974**, *8*, 85. Dougherty, R. C.; Dalton, J.; Roberts, J. D. *Ibid.* **1974**, *8*, 77. This ion–dipole stabilization shows rather small variation for complexes of the types discussed here. For example, for $F^-\cdot CH_3F$ it is 13.2 kcal/mol and for $H^-\cdot CH_3F$ it is 12.2 kcal/mol (computed in ref 2a). Some of this stabilization may be counteracted by the weak 2-electron interaction (as well as other interactions) between N· and $(H_3C\therefore X)^-$ at the encounter distance so that eq 7 is a good approximation for the encounter distance.

(25) (a) The connection between electron transfer and nucleophilic attacks on peroxides was described in terms of a DA–D^+A^- crossing recently by: Walling, C. *J. Am. Chem. Soc.* **1980**, *102*, 6854–6855. The S_N2 reaction was suggested to have "an electron-transfer component" by: Bank, S.; Noyd, D. A. *Ibid.* **1973**, *95*, 8203–8205. (b) Note the excited intermediate above the S_N2 transition state in Figure 1 also involves electron transfer from the nucleophile to the substrate [$\psi^* \sim 2^{-1/2}$(I–II)].

(26) ΔH is an approximation for the energy difference of the reactants' and products' encounter complexes. This is a good approximation since the ion–dipole stabilization of most complexes (of the types discussed here) differ by ≤4 kcal/mol.[24] See also ref 1f,g.

(27) This maxim is from the closing sentences of: Hoffmann, R. In "Aspects de la Chimie Quantique Contemporaine"; Daubel, R., Pullman, A., Eds.; CNRS: Paris, 1971.

of a stable 2-electron bond with the nucleophile (eq 3 and 5). These two effects compete with each other. As long as the 3-electron bond in A^- has not been localized, the new 2-electron bond between the nucleophile and the substrate cannot be fully realized. In order to explain this point, let us first consider $(D^+A^-)_r$ and inspect the $(H_3C\therefore X)^-$ 3-electron bond. These types of 3-electron bonds are unstable.[17,18,28] Their only stabilizing interaction is contributed by the delocalization or the resonace between the two valence forms:

$$(H_3C\therefore X)^- = a(H_3C\cdot\ :X^-) \leftrightarrow b(H_3C^-:\ \cdot X) \qquad (8)$$

As eq 8 shows, the extent of this resonance stabilization depends on the similarity of the electron affinities of $H_3C\cdot$ and $X\cdot$. The closer they are, the more delocalized and resonance stabilized the 3-electron bond. During the descent of D^+A^- (Figure 1b), this 3-electron bond is gradually localized as $H_3C\cdot\ :X^-$, thereby losing its resonance energy. Therefore, an increase in the resonance stabilization of the $(H_3C\therefore X)^-$ 3-electron bond will have a *retarding* effect on the descent of $(D^+A^-)_r$.

The gradual formation of the N–C bond comes about from two sources: from the 2-electron interaction in the $N\cdot\ \cdot CH_3\ :X^-$ VB form (I)[11b] within $(D^+A^-)_r$ and by the interaction of this form (I) with the carbenium configuration $N^-:\ ^+CH_3\ :X^-$ (III), as was discussed with reference to eq 5. Since $(D^+A^-)_r$ reads

$$(D^+A^-)_r = a(N\cdot\ \cdot CH_3\ :X^-) \leftrightarrow b(N\cdot\ :^-CH_3\ \cdot X) \qquad (9)$$

the weight, a of VB form I diminishes as the $(H_3C\therefore X)^-$ bond becomes more delocalized, and therefore, the 2-electron stabilization ($N\cdot\ \cdot CH_3$) as well as the mixing with $N^-:\ ^+CH_3\ :X^-$ progress slowly. This means that a strongly delocalized $(H_3C\therefore X)^-$ 3-electron bond also retards the formation of the $N–CH_3$ bond and thereby slows down the descent of $(D^+A^-)_r$ even further. The same considerations apply equally well to $(D'^+A'^-)_p$; i.e., the more delocalized the $(H_3C\therefore N)^-$ 3-electron bond the slower the descent of $(D'^+A'^-)_p$. In summary the extent of delocalization and the resonance stabilization of the $(H_3C\therefore X)^-$ and $(H_3C\therefore N)^-$ 3-electron bonds have a considerable impact on S_N2 reactivity; *the more delocalized the 3-electron bonds the slower the descent of the D^+A^- curves (in the region prior to their crossing) and the larger the fraction of the initial energy gap ($I_D - A_A$) entering the activation barrier (for a given gap).*

Let us now shift our attention to two ground anchor points of Figure 1b, $(DA)_r$ and $(D'A')_p$. These two points differ in energy by the reaction enthalpy, ΔH, and thus provide us with additional information about the barrier height. Strictly speaking, when all other factors are equal i.e., the initial gap ($I_D - A_A$) and the extent of delocalization of the 3-electron bonds, only then can one predict that an increase in reaction exothermicity will be accompanied by a decrease of the reaction barrier as shown schematically in Figure 4. The case shown in Figure 4 corresponds to the commonly described Bell–Evans–Polanyi[8] behavior. As one can see, in such cases an increase in reaction exothermicity increases the rate of descent of $(D^+A^-)_r$ (relative to $(D'^+A'^-)_p$), thereby allowing a smaller fraction of the initial energy gap ($I_D - A_A$) to enter the activation barrier. We shall discuss such cases and analyze in greater detail the role of reaction exothermicity in a separate section.

The fourth reactivity factor is the degree of avoided crossing which we indicated in Figure 1b by $|\beta|$. We expect this parameter to show the least sensitivity to variations in structure, and therefore, it will be assumed as constant within our scheme. Although this is not strictly correct, we are compelled to do so if we wish to treat a large body of data without increasing the number of reactivity parameters beyond reason. As we shall see later, when we inspect the experimental data, this assumption does not appear to impair the predictive ability of the model to a significant extent.

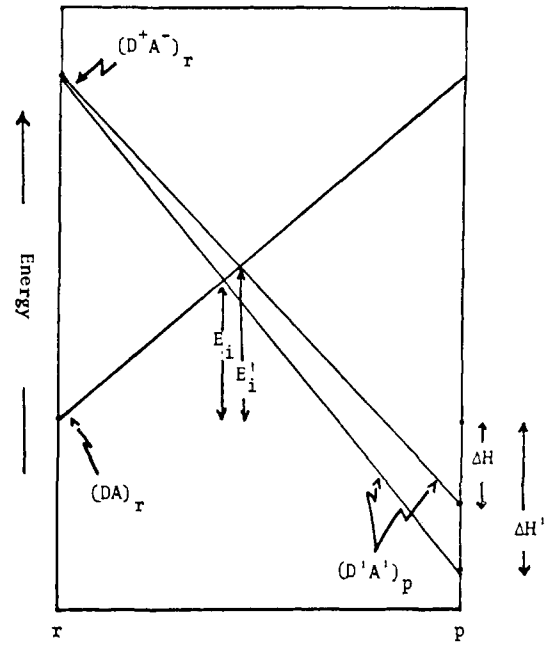

Figure 4. Schematic description of the effect of reaction exothermicity (ΔH) on the energy of the intersection point. The intersection point will be lower in energy ($E_i < E_i'$) as reaction exothermicity increases ($|\Delta H| < |\Delta H'|$).

The foregoing discussion suggests that one can write a general expression for the S_N2 barrier in the following compact manner:

$$E^* = r(I_D - A_A) - |\beta| \qquad (10)$$

where $I_D - A_A$ is the initial energy gap (Figure 2a), and r is a slope parameter which determines what fraction of $I_D - A_A$ enters the activation barrier. β is the avoided crossing constant. Equation 10 suggests that the ensemble of the S_N2 reactions will be subdivided into families with a common slope parameter, r. Within each such family reactivity will be determined by the $I_D - A_a$ parameter, and hence the reactivity within the family can be called *electron-transfer controlled.*[29] In comparisons between families, both $I_D - A_A$ and r will determine reactivity. Those series whose reactivity will be dominated by r will be called *slope controlled.* In the following sections we shall show that these two trends indeed manifest themseleves in the experimental data.

III. Estimation of Reactivity Parameters

This section will be devoted to the estimation of the reactivity parameters $I_D - A_A$, r, and β which we discussed in the previous section. The approach we adopt is to relate the various parameters within a thermochemical cycle whose individual steps are based on our proposed model for the S_N2 reaction. The entire cycle is presented in eq 11.

$$N^-:\ + CH_3–X \rightarrow N\cdot^* + [(CH_3\therefore X)^-]^* \quad \Delta H_1 = I_{N:} - A_{CH_3X} \qquad (11a)$$

$$N\cdot^* \rightarrow N\cdot \quad \Delta H_2 = R_{N\cdot}\ (\leq 0) \qquad (11b)$$

$$[(CH_3\therefore X)^-]^* \rightarrow \cdot CH_3 + :X^- \quad \Delta H_3 = R_{C\therefore X} \qquad (11c)$$

$$N\cdot + \cdot CH_3 \rightarrow N–CH_3 \quad \Delta H_4 = -H^0_{N-C} \qquad (11d)$$

$$N^-:\ + CH_3–X \rightarrow X^-:\ + N–CH_3$$

(28) See, for example, optimized structures of CH_3Cl^- and CH_3F^- in: Clark, T. *J. Chem. Soc., Chem. Commun.* **1981**, 515–516. (b) See also Salem's work in ref 22. (c) Reference 18. (d) Sprague, E. D.; Williams, F. *J. Chem. Phys.* **1971**, *54*, 5425. (e) Mishra, S.; Symons, M. C. R. *J. Chem. Soc., Perkin Trans. 2* **1973**, 391. (f) Fujita, Y.; Katsu, T.; Sato, M.; Takahashi, K. *J. Chem. Phys.* **1974**, *61*, 4307. (g) Sprague, E. D.; Takeda, K.; Wang, J. T.; Williams, F. *Can. J. Chem.* **1974**, *52*, 2840.

(29) Electron-transfer-controlled reactions are actually those which follow HOMO–LUMO energy gap considerations within the PMO framework. For applications to S_N2, see, for example: (a) ref 9. (b) Hudson, R. F. *Angew. Chem., Int. Ed. Engl.* **1973**, *12*, 36–56. (c) Karton, Y.; Pross, A. *J. Chem. Soc., Perkin Trans. 2* **1979**, 857–861. (d) Epiotis, N. D.; Cherry, W. R.; Shaik, S.; Yates, R.; Bernardi, F. *Top. Curr. Chem.* **1977**, *70*, 12–14. (e) Klopman, G. *J. Am. Chem. Soc.* **1968**, *90*, 223. (f) Fleming, I. "Frontier Orbitals and Organic Chemical Reactions"; Wiley: New York, 1976, pp 37–40.

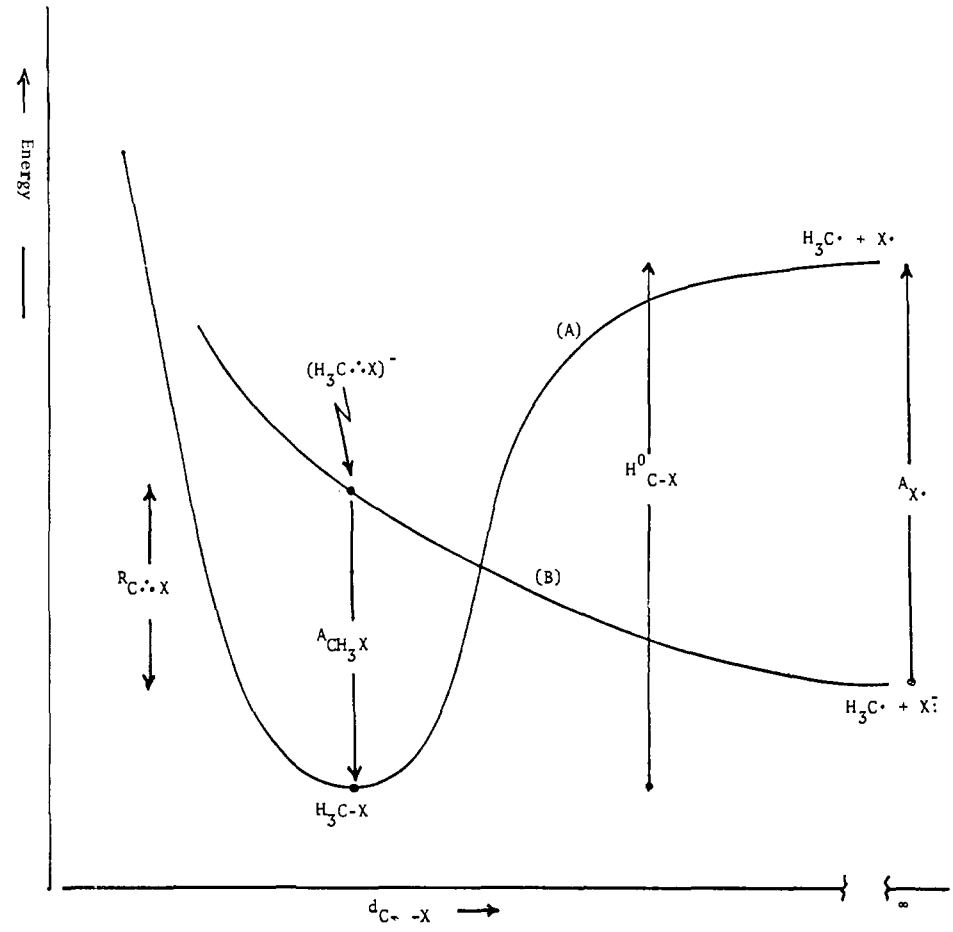

Figure 5. Relation of the substrate electron affinity A_{CH_3X} (see eq 14) to the 2-electron bond strength (H^0_{C-X}), the X electron affinity ($A_{X\cdot}$), and the 3-electron bond reorganization energy ($R_{C\cdot\cdot X}$). Curve A describes the H_3C-X bond while curve B corresponds to the $(H_3C\cdot\cdot X)^-$ form.

The first step (a) in the cycle involves an electron jump from the nucleophile N^-: to the substrate CH_3X. The second step involves the relaxation of N· from its geometry in N^-: to its new geometry. The asterisk denotes the nonrelaxed geometry and indicates that in the first process 11a the electron is transferred vertically without any change in the geometries of N^-: and CH_3X. The energy involved in this first step, $I_{N:} - A_{CH_3X}$, corresponds to the desired energy gap between the anchor points of the intersecting curves in Figure 1b. Thus A_{CH_3X} is not an electron affinity in the strict sense of the thermodynamic definition; rather, it is related to the vertical transition $CH_3-X + e^- \rightarrow (H_3C\cdot\cdot X)^-$. $R_{N\cdot}$ (process 11b) is the reorganization energy involved in relaxing N·* to its most stable geometry. This term equals zero when N is a monoatomic entity. However, this is not the case when N is a molecular entity such as OH, where one expects some geometry differences between HO^- and HO·. Therefore, $R_{N\cdot}$ is expected to be a finite negative quantity for a polyatomic N^-:. The third step (11c) in the cycle involves the reorganization of the 3-electron bonded entity $[(H_3C\cdot\cdot X)^-]^*$ from the geometry of CH_3X all the way to relaxed CH_3 and X^-:. The reorganization energy, $R_{C\cdot\cdot X}$, corresponding to this process provides indirect information regarding the resonance stabilization and the degree of delocalization of the 3-electron bond. The fourth and the final step (11d) of the cycle is the N–C 2-electron bond formation whose energy is denoted by H^0_{N-C}.

Summation of the individual enthalpy terms of eq 11 establishes a link between the reactivity parameters and the reaction enthalpy:

$$I_{N:} - A_{CH_3X} = \Delta H + H^0_{N-C} - R_{N\cdot} - R_{C\cdot\cdot X} \qquad (12)$$

For the identity reaction (i.e., for N = X), where $\Delta H = 0$ we obtain eq 13

$$A_{CH_3X} = I_{X:} + R_{X\cdot} - H^0_{C-X} + R_{C\cdot\cdot X} \qquad (13)$$

Combining $I_{X:} + R_{X\cdot}$ as the adiabatic X· electron affinity ($A_{X\cdot}$)[30] the substrate electron affinity becomes

$$A_{CH_3X} = A_{X\cdot} - H^0_{C-X} + R_{C\cdot\cdot X} \qquad (14)$$

The relationship between these terms is shown in Figure 5, which illustrates how the substrate acceptor ability is determined by the balance between the X· electron affinity, the 2-electron bond strength (H^0_{C-X}) and the reorganization energy of the 3-electron bond ($R_{C\cdot\cdot X}$). Since most $(C\cdot\cdot X)^-$ 3-electron bonds are expected to be unstable with respect to decomposition,[18,28] the reorganization term ($R_{C\cdot\cdot X}$) is taken as a negative quantity in Figure 5.

In order to complete our knowledge of the reactivity parameters, we need to estimate $R_{C\cdot\cdot X}$[31] and determine the extent of delocalization for various 3-electron bonds. *In principle*, this is not difficult since all we need to know are the energies of the localized forms, $E_1(C\cdot\ :X^-)$ and $E_2(C^-:\ \cdot X)$, as well as their interaction matrix element, H_{12}, at the C– –X contact of the CH_3X molecule. Thus

$$E[(C\cdot\cdot X)^-] = \tfrac{1}{2}\{(E_1 + E_2) - |[(E_1 - E_2)^2 + 4H_{12}^2]^{1/2}|\} \qquad (15)$$

(30) The quantity $|R_{X\cdot}|$ is the difference between the vertical and adiabatic $A_{X\cdot}$ values (we use here $I_{X:}$ to denote vertical $A_{X\cdot}$). This quantity is expected to be small for localized anions. For example, photodetachment experiment for CH_3O^- yields $A_{CH_3O\cdot} \leq 36.7 \pm 1.0$ kcal/mol. This value is likely to be vertical (Reed, K. J.; Brauman, J. I. *J. Am. Chem. Soc.* **1975**, *97*, 1625). On the other hand, ΔH_f data[16] yield $A_{CH_3O\cdot} = 31 \pm 2.3$ kcal/mol, which is likely to be an adiabatic value. Thus the difference is quite small $|R_{CH_3O\cdot}| \sim 5.7 \pm 3.3$ kcal/mol. For general considerations, see: Janousek, B. K.; Brauman, J. I. In "Gas Phase Ion Chemistry"; Bowers, M. T., Ed.; Academic Press: New York, 1979; Vol. 2, Chapter 10.

(31) Another way is to assume that $(I_{N:} - A_{RX}) - (I_{X:} - A_{RN}) \sim \Delta H$ (see Figure 1b). This assumption leads to the following expression for differences in 3-electron bond reorganization energies: $R_{C\cdot\cdot X} - R_{C\cdot\cdot N} = I_{N:} - I_{X:} \equiv A_{N\cdot} - A_{X\cdot}$. This expression leads to correct predictions about the relative resonance stabilization of 3-electron bonds.

and the mixing coefficients a_1 and a_2 of the two forms are

$$a_{1,2} = \tfrac{1}{2}\{1 \pm [\Delta/(\Delta^2 + 4)^{1/2}]\};\ \Delta = |(E_1 - E_2)/H_{12}| \qquad (16)$$

In practice this task is difficult, since we do not know E_1, E_2, or H_{12}. Thus, we must make some assumptions which will enable us to estimate these three variables for a series of X's.

Let us start with E_1 and E_2. As the two fragments (H_3C and X) approach one another up to their distance in the neutral molecule (CH_3X), the two localized forms $C\cdot :X^-$ and $C^-: \cdot X$ are destablized by *exchange repulsion* as shown in Figure 6. This exchange repulsion is due to the overlap of two electrons which have the same spin, one residing on X and the other in C.[12,17e] The most straightforward way to estimate the exchange repulsion is to equate its absolute magnitude with the *exchange stabilization* which arises from the overlap of two singlet paired electrons, one on C and one on X.[32] This 2-electron exchange stabilization has a similar expression to the 3-electron exchange repulsion, both owing their origins to the $|2\beta_{CX}S_{CX}|$ term.[11b,12]

The 2-electron exchange stabilization is the "pure" covalent contribution to the C–X bond energy, and can be estimated thermochemically as the geometric mean of the covalent bond energies of the C–C and X–X bonds, using the Pauling's relation.[11b]

$$H^0_{C\text{-}X}(\text{covalent}) \sim (H^0_{C\text{-}C}H^0_{X\text{-}X})^{1/2} \qquad (17)$$

Thus, this term may be used as an estimate of the 3-electron exchange repulsion in each of the two localized forms. Accordingly, E_1 and E_2 relative to the separate fragments $C\cdot + :X^-$ become (Figure 6)

$$E_1 \sim (H^0_{C\text{-}C}H^0_{X\text{-}X})^{1/2} = E_1(C\cdot :X^-) - E(C\cdot + :X^-) \qquad (18)$$

$$E_2 \sim (H^0_{C\text{-}C}H^0_{X\text{-}X})^{1/2} + A_{X\cdot} - A_{C\cdot} \sim E(C^-: \cdot X) - E(C\cdot + :X^-) \qquad (19)$$

where $A_{X\cdot}$ and $A_{C\cdot}$ are the electron affinities of $X\cdot$ and $\dot{C}H_3$ (see Figure 6).

Let us now estimate the value of H_{12}. Since the two localized forms of the 3-electron bond differ by one electron shift, using an effective one-electronic Hamiltonian, one obtains a simple expression for H_{12} (eq 20)

$$|H_{12}| = |\langle C\cdot :X|\hat{H}|C: \cdot X\rangle| = |\langle\phi_C|\hat{H}_{eff}|\phi_X\rangle| = |\beta_{CX}| \qquad (20)$$

If we now equate our estimated 3-electron exchange repulsion with the quantum mechanical term $|2\beta_{CX}S_{CX}|$, we have a way of estimating the matrix element as

$$|\beta_{CX}| \sim (1/2S_{CX})\ (H^0_{C\text{-}C}H^0_{X\text{-}X})^{1/2} \qquad (21)$$

Now eq 15 becomes

$$E[(C\therefore X)^-] = (H^0_{C\text{-}C}H^0_{X\text{-}X})^{1/2} + \tfrac{1}{2}\{(A_{X\cdot} - A_{C\cdot}) - |[(A_{X\cdot} - A_{C\cdot})^2 + (H^0_{C\text{-}C}H^0_{X\text{-}X})/S_{CX}^2]^{1/2}|\} \qquad (22)$$

where $E[(C\therefore X)^-]$ is the energy of the 3-electron bond relative to the separated ($H_3C\cdot + :X^-$) fragments as indicated in Figure 6. This equation contains known thermochemical quantities, and hence, it allows the estimation of the reorganization energy using the identity $R_{C\therefore X} = -E[(C\therefore X)^-]$ and the extent of delocalization of the 3-electron bonds, provided we know the overlap values, S_{CX}, for various bonds. Since we do not know the identity of the hybrids on H_3C and X, we have employed a standard value of overlap (S_{CX} = 0.5) which appears to be a satisfactory choice from most C–X bonds.[33] Nonetheless, in order to check the sensitivity of the trends to the value of S_{CX}, we have also performed calculations with a range of overlaps corresponding to different degrees of hybridization.

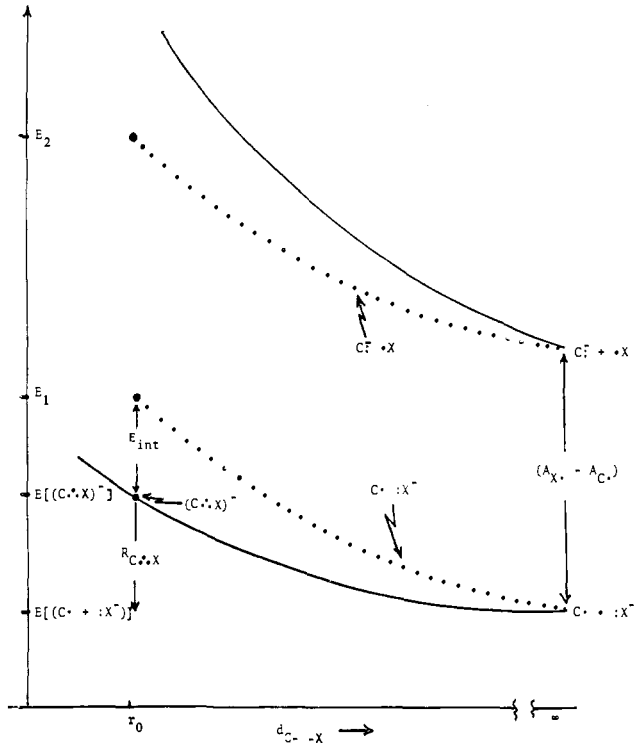

Figure 6. Interaction diagram describing the formation of the 3-electron bond $(C\therefore X)^-$ at the C–X distance (r_D) of the neutral molecule H_3C–X. The dotted curves describe the destabilization of the VB forms $C\cdot :X^-$ and $C^-: \cdot X$ as the C– –X distance (d) shortens. The solid curves describe the resulting states after interaction of the VB forms. The lower solid curve describes the formation of the (unstable) 3-electron bond, $(C\therefore X)^-$. E_{int} is the 3-electron bond resonance energy at r_0. The energies of the VB forms and states (eq 18–20, 22) are indicated on the energy axis. $A_{X\cdot} - A_{C\cdot}$ is the energy gap between the two VB forms.

Before presenting the results we would like to make one more comment about eq 22. One should not expect this equation to produce good absolute values (which are difficult to verify in any case since neither valence electron affinities nor 3-electron bond reorganization energies are available for these unstable species). What we expect is that the equation will reproduce the correct trends in these quantities. In order to check this point we have selected two molecules whose electron affinitites are experimentally known, F_3C–I and F_3C–Br,[34a] and have calculated[34b] their $R_{C\therefore I}$ and $R_{C\therefore Br}$ values using the standard overlap S_{CX} = 0.5. Having the $R_{C\therefore X}$ values (–2.73 and –6 kcal/mol, respectively) we have calculated (eq 14) the difference in their electron affinities ($A_{F_3CI} - A_{F_3CBr}$) to be 13.5 kcal/mol, while the experimental difference is ~15.1 ± 4.6 kcal/mol.[34c] This result gives us confidence that *eq 22 together with the thermochemical relation in eq 14* are indeed capable of reproducing the correct trends in the reactivity parameters, and we can turn to inspect the results for CH_3X systems in Table I. Table I presents three sets of results for

(32) We have checked this assumption for $H^-: \cdot H$ and $H\cdot \cdot H$ using STO-3G integrals. As long as the AO overlap does not exceed 0.5, the assumption is a good one. Thus at 1 Å (S_{HH} = 0.5) the 3-electron destabilization is ~97 kcal/mol, whereas the 2-electron stabilization is 91 kcal/mol, and for smaller S_{HH} values they are equal. At shorter distances when $S > 0.6$ the exchange destablization exceeds the exchange stabilization as can be expected from inclusion of overlap in the normalization constants. Since the Pauling relation (eq 17) most likely overestimates the 2-electron interaction, it is expected to be a fairly good approximation for the 3-electron interaction.

(33) For example, for $C(sp^3)$–$X(sp^3)$, S_{CX} overlaps are 0.4926, 0.5788, and 0.5427 for X = F, Cl, O, respectively, while for $C(sp^3)$–$X(sp^5)$ they are 0.4805, 0.5611, and 0.5193 in respective order. All AO overlaps are obtained over Slater AOs.

(34) (a) Compton, R. N.; Reinhardt, P. W.; Cooper, C. D. *J. Chem. Phys.* **1978**, *68*, 4360. (b) A_{CF_3} was taken from: Richardson, J. H.; Stephenson, L. M.; Brauman, J. I. *Chem. Phys. Lett.* **1979**, *30*, 17. $H^0_{C\text{-}X}$(covalent) for C–I and C–Br (eq 17) were calculated from bond strength data using $H^0_{C\text{-}C}$ = 88 kcal/mol; $H^0_{I\text{-}I}$ = 36 kcal/mol, and $H^0_{Br\text{-}Br}$ = 46 kcal/mol. (c) A value of $S_{Cl} = S_{CBr}$ = 0.4 reproduces also the absolute values of $A_{CF_3\text{-}Br}$ and $A_{CF_3\text{-}I}$. Such a value for the overlap is expected if the C–X bonds in the anions are longer than in the neutrals.

Table I. Calculated A_{CH_3X} (kcal/mol) and Degree of Delocalization (a_2^2) of 3-Electron Bonds $(H_3C\therefore X)^-$ [a]

		I[b]		II[c]		III[d]			
	X	A_{CH_3X}	a_2^2	A_{CH_3X}	a_2^2	A_{CH_3X}	a_2^2	$A_{X\cdot}$[e]	H^0_{C-X}[e]
(1)	F	−58	0.22	−59	0.22	−55	0.24	76	108
(2)	Cl	−30	0.25	−39	0.22	−37	0.23	83	84
(3)	Br	−21	0.25	−28	0.22	−27	0.23	78	71
(4)	I	−10	0.24	−16	0.21	−15	0.22	71	56
(5)	HO	−65	0.35	−70	0.34	−67	0.35	44	91
(6)	CH_3O	−63	0.38	−67	0.37	−65	0.37	31	81
(7)	CF_3CO_2	−16	0.15	−18	0.14	−16	0.14	103	88
(8)	CH_3S	−47	0.37	−57	0.34			44	73
(9)	NC	−69	0.31	−99	0.26	−95	0.27	90	122
(10)	HCC	−90	0.40	−124	0.36	−120	0.37	47	117
(11)	H	−93	0.46	−119	0.44			19	104
(12)	H_2N	−70	0.45	−83	0.43	−82	0.44	20	81

[a] A_{CH_3X} is calculated from eq 14 using $R_{C\therefore X}$ values. $R_{C\therefore X}$ is calculated from eq 22. a_2^2 is calculated from eq 16. See ref 35 for thermochemical data. [b] $S_{CX} = 0.5$. [c] All X's are sp^3 hybridized except for X = NC, HCC (sp). C is sp^3 throughout. [d] All X's are sp^5 hybridized except for X = NC, HCC (sp^3). C is sp^3 throughout. [e] These values are rounded off and are displayed for comparison.

valence electron affinities, A_{CH_3X}, and extent of delocalization of 3-electron bonds. The latter quantity is indicated by a_2^2, which is the square of the mixing coefficient of the carbanionic form $C\therefore X^-$ (eq 16). The three sets were obtained with three different choices of the S_{CX} overlap in eq 22.[33] In the last set we have increased the amount of p character in the hybrids on X in accord with chemical intuition that X's like F, Cl, O, etc., use hybrids with greater p character for bonding. In the last two columns we have listed X's electron affinities ($A_{X\cdot}$) and 2-electron bond energies which were taken from standard thermochemical sources.[35]

Let us first consider the values of the valence electron affinities. Inspection of Table I reveals that the acceptor ability of various σ bonds follow the order $A_{CH_3-H} \sim A_{CH_3-CCH} < A_{CH_3-CN} < A_{CH_3-NH_2} < A_{CH_3-OH} \leq A_{CH_3-OCH_3} < A_{CH_3-F} < A_{CH_3-SCH_3} < A_{CH_3-Cl} < A_{CH_3-Br} < A_{CH_3-OCOF_3} < A_{CH_3-I}$. Note that (with one exception A_{CH_3-H} vs. A_{CH_3-CCH}) this order is not dependent on the choice of the overlap.

The origins of this trend can be revealed by considering the $A_{X\cdot}$ and H^0_{C-X} values in the light of Figure 5. For the methyl halides (runs 1–4) the trend is $A_{CH_3-I} > A_{CH_3-Br} > A_{CH_3-Cl} \gg A_{CH_3-F}$ which is in accord with the trend in their reduction potentials,[36] and other criteria such as the energy level of the corresponding σ^*_{CX} MOs.[29] Inspection of Table I reveals that the halogens have approximately equal $A_{X\cdot}$ values, and our calculations show that they also have approximately equal 3-electron bond reorganization energies ($R_{C\therefore X}$ = −25, −28, −30, and −26 kcal for X = I, Br, Cl, and F). It follows then, in the light of Figure 5, that the trend in their A_{CH_3X} value is set by the 2-electron bond strength (H^0_{C-X}), and that *the strongest C–X bond will also be the worst acceptor.* This trend is expected whenever one compares A_{CH_3X} values when X is varied down the column of the periodic table, as can be judged from other calculated trends (runs 5, 6, 8); $A_{CH_3-SCH_3} > A_{CH_3-OCH_3}$ and $A_{CH_3-SCH_3} > A_{CH_3-OH}$. When one compares A_{CH_3X} values as X is varied along a row of the periodic table or at random, the situation becomes more complex and the trends are set by $A_{X\cdot}$, H^0_{C-X}, and $R_{C\therefore X}$ together. If we, for example, compare the acceptor abilities of CH_3–OR (R = H, CH_3) to those of methyl halides, we find that the poorer acceptor abilitites of CH_3–OR originate from the combination of low $A_{RO\cdot}$ and fairly strong 2-electron bonds. Similarly, the better acceptor ability of H_3C–$OCOCF_3$ relative to H_3C–OH or H_3C–OCH_3 (runs 5–7) arises from the much larger X electron affinity ($A_{X\cdot}$) of CF_3CO_2. Finally, CH_3–CN and CH_3–CCH (runs 9, 10) are poor electron acceptors mainly because of their very strong 2-electron bonds, while $A_{CH_3-CN} > A_{CH_3-CCH}$ mainly because of the fact that $A_{NC\cdot} > A_{HCC\cdot}$.

Let us now turn to consider the extent of delocalization of the 3-electron bonds in Table I. This variable is given by a_2^2 which amounts to the contribution of the carbanionic form $C^-\!:\cdot X$ to the description of the 3-electron bond, $(C\therefore X)^-$. Hereafter, we shall refer to the extent of delocalization as "strength" so that delocalized bonds will be termed "strong" while localized ones will be referred to as "weak". Table I predicts a clear cut demarcation into two groups of 3-electron bonds. The first group is that of the "weak" 3-electron bonds which belong to X's with high $A_{X\cdot}$, i.e., to X = F, Cl, Br, I, and CF_3CO_2 (runs 1–4, 7). The 3-electron bonds belonging to this group are virtually localized having ≥0.75 of the extra electron on X, and their resonance stabilization (E_{int} in Figure 6) is quite small being ~18–40 kcal/mol. The second group is that of the "strong" 3-electron bonds which belong to X's with low $A_{X\cdot}$, i.e., to X = HO, CH_3O, CH_3S, H, NH_2, and HCC (runs 5, 6, 8, 10–12). The 3-electron bonds belonging to this group are heavily delocalized having ≥0.4 of the extra electron on the carbon, and their resonance energies are quite high (47–90 kcal/mol). The $(C\therefore CN)^-$ bond falls somewhere in between the two groups. These trends in the 3-electron bonds "strengths" have an inherent chemical logic to them, and they follow the theoretical considerations[17] in section II.

Having estimated the key parameters which determine the barrier height in S_N2 reactions, together with literature $I_{N\cdot}$ (recall $I_{N\cdot} \sim A_{N\cdot}$) values, we can now discuss reactivity trends in gas-phase S_N2 reactions.

IV. The Barrier in the S_N2 Identity Reaction

The identity exchange $X^-\!: + CH_3X \rightarrow XCH_3 + X^-\!:$ is a unique set within the ensemble of the S_N2 reactions. It occurs with no thermodynamic driving force, and hence, its barrier is, what one may call, intrinsic. The idea of intrinsic barriers which originated in the Marcus theory[37] of electron transfer is gradually becoming a central concept of physical organic chemistry,[38] and hence understanding the trends in the barriers of identity reactions is a major step along the path toward understanding S_N2 reactivity as a whole.

Recent gas-phase results by Pellerite and Brauman[1g] enabled the estimation of gas-phase barriers for a few identity reactions. Their results were very similar to existing solution data.[3] Within the halides Pellerite and Brauman found a large barrier for X^-:

(35) (a) Bond energies were taken from: Sanderson, R. T. "Chemical Bonds and Bond Energy"; Academic Press: New York, 1976. Benson, S. W. *J. Chem. Educ.* **1965**, *42*, 502–518 ref 1e. (b) $I_{X\cdot}$ ($A_{X\cdot}$) values were taken from: Chen, E. C. M.; Wentworth, W. E. *Ibid.* **1975**, *52*, 486–489 (for halides). Hiraoka, K.; Yamdagni, R.; Kebarle, P. *J. Am. Chem. Soc.* **1973**, *95*, 6833–6835 (CF_3CO_2); ref 1e (HO, CH_3O, CH_3S, NC, HCC, H, H_2N). Ellison, C. B.; Engelking, P. C.; Lineberger, W. C. *Ibid.* **1978**, *100*, 2556 (CH_3).

(36) Weinberg, N. L., Ed. "Techniques of Electro-Organic Synthesis"; Wiley: New York, 1975; Vol. 5, Part II, pp 827–839.

(37) (a) Marcus, R. A. *Annu. Rev. Phys. Chem.* **1964**, *15*, 155. (b) Marcus, R. A. *J. Phys. Chem.* **1968**, *72*, 891, 4249. (c) Brunschwig, B. S.; Logan, J.; Newton, M. D.; Sutin, N. *J. Am. Chem. Soc.* **1980**, *102*, 5798–5809.

(38) For applications, see: (a) ref 3a, 1g. (b) Murdoch, J. R. *J. Am. Chem. Soc.* **1972**, *94*, 4410–4418. (c) Murdoch, J. R. *Ibid.* **1980**, *102*, 71–78. (d) Kreevoy, M. M.; Oh, S. *J. Am. Chem. Soc.* **1973**, *95*, 4805–4810. (e) Agmon, N. *Ibid.* **1980**, *102*, 2164.

Table II. Reactivity Factors and Barriers (E^*) for Identity Reactions (energies in kcal/mol) $X^-: + CH_3-X \rightarrow X-CH_3 + :X^-$

	reactivity factors[a]			E^*	
	X	$I_{X:} - A_{CH_3X}$	a_2^2	gas phase[b]	soln (H_2O)[d]
(1)	F	134	0.22	19.5 ± 1.0 (26.2); 20[c]	31.8 (30.7)
(2)	Cl	113	0.25	11.6 ± 1.8 (~10.2)	26.5 (26.6)
(3)	Br	99	0.25	9.7 ± 1.9 (~11.2)	23.7 (22.5)
(4)	I	81	0.24		23.2 (22.0)
(5)	CF_3CO_2	119	0.15	19.3 ± 2.6	34.7[e]
(6)	HO	109	0.35	29.0 ± 1.1	39.4; 41.8
(7)	CH_3O	94	0.38	27.0 ± 2.6 (26.6)	
(8)	CH_3S	91	0.37	23.5 ± 1.4	
(9)	NC	159	0.31	36.6 ± 3.2	50.9
(10)	HCC	137	0.40	38.9 ± 2.3	
(11)	H	112	0.46	48.3 ± 2.7; 63[c]	
(12)	H_2N	90	0.45	19.2 ± 2.5	

[a] A_{CH_3X} and a_2^2 are taken from set I in Table I. $I_{X:}$ (=$A_{X\cdot}$) values are from ref 35b. [b] Values in parentheses from ref 1g. For others see ref 40. [c] From ref 2a (by ab initio). [d] Values from ref 3a. Those in parentheses from ref 3b. [e] This value is for $X^-: = CH_3SO_3^-$.

$= F^-$ ($E^* \geq 20$ kcal/mol), whereas small barriers were estimated for $X^- = Cl^-, Br^-$ ($E^* \sim 10$ kcal/mol). Similarly, large barriers were found for $X^-: = CH_3O^-$, t-BuO^- ($E^* \geq 20$ kcal/mol). Thus, Pellerite and Brauman[1g] established for the first time that the sluggish leaving group ability of F^- and CH_3O^- are intrinsic properties independent of solvation effects. Yet another surprising trend was that reactivity in the identity exchange series, in the gas phase as well as in solution,[3a] followed the leaving group ability, *despite the fact that, at the same time, nucleophilicity itself was changing drastically*.[39]

These trends require an explanation. Equation 10 and the preceding discussion in Section II predict that the barrier for an identity reaction will be determined by two variables: (1) The initial gap, $I_{X:} - A_{CH_3X}$, of the two intersecting curves (1st reactivity rule) and (2) the slopes of descent of the curves in the region prior to their intersection (2nd reactivity rule, Figure 3), which in the case of identity reactions where $\Delta H = 0$ will be dominated by the "strength" (i.e., degree of delocalization) of the 3-electron bond $(C\therefore X)^-$. It follows that we can, in principle, subdivide reactivity trends, in the ensemble of identity reactions, into two types: (1) *Electron-transfer-controlled* series in which reactivity is dominated by the donor–acceptor abilities of the reactants ($I_{X:} - A_{CH_3X}$) and (2) *3-electron bond-controlled* series in which reactivity is dominated by variations in the 3-electron bond "strength" of the reactants.

Let us not inspect the experimental data in the light of our proposed reactivity parameters. Using the data in Table I we have estimated the electron transfer or energy gap $I_{X:} - A_{CH_3X}$ variable for a variety of identity reactions. These values are presented in Table II along with the values (a_2^2) of the 3-electron bond strength variable. In the third column of Table II we present the calculated gas-phase barriers of Pellerite and Brauman[1g] and other barriers calculated[40] from data in papers by Brauman[1] and Bohme[1] as well as a few theoretical barriers.[2a,f] These gas-phase data refer to the central barrier separating the loose ion–dipole complexes, $X^-:\cdots CH_3X \rightarrow XCH_3\cdots X^-:$. In the last column of Table II we present aqueous solution data obtained by Albery and Kreevoy[3a] and McLennan.[3b]

The data in Table II exhibit a clear-cut division of the reactions into two sets. The first set includes all the reactions with the "weak" (i.e., localized) 3-electron bond, $C\therefore X$. These are runs 1–5 for which the 3-electron bond is virtually localized (a_2^2 = 0.15–0.25), and we may incorporate X = NC to this group. The second set (runs 6–8, 10–12) involves all the reactions with the "strong" or relatively delocalized (a_2^2 = 0.35–0.46) 3-electron bond. Within the former set, with the "weak" 3-electron bonds, the reaction barriers increase with $I_{X:} - A_{CH_3X}$ and hence this set is *electron-transfer controlled*, namely, its reactivity responds to the donor–acceptor abilitites of the reactants. A special set within this group is the set of halide exchange (runs 1–4). Along this series the 3-electron bond "strength" is virtually constant, and therefore we can really ascribe the reactivity trend to just variations in the donor–acceptor ability ($I_{X:} - A_{CH_3X}$). Since $I_{X:} = A_{X\cdot}$ and the $A_{X\cdot}$ values for the halogens are similar (see Table I), it follows that the substrate electron affinity is the major factor which dominates the reactivity in the halide exchange reactions. Therefore, *we conclude that the poor leaving group ability exhibited by F^- has its origins in the poor acceptor ability of* CH_3F, which in turn originates in the strong C–F bond (Table I). Similarly, if we examine the reaction of NC^-, we reach the same conclusion, i.e., the poor acceptor ability of CH_3–CN (strong C–CN bond) is responsible for the low reactivity of NC^- exchange. The same trends are observed in solution. What the solvent appears to do is simply to increase the reaction barrier. This arises from an increase in the $I_{X:} - A_{CH_3X}$ energy gap owing to enhanced differential solvation of X^-: relative to $(H_3C\therefore X)^-$.

The second set in Table II includes all the reactions with relatively strong $(C\therefore X)^-$ bonds (runs 6–8, 10–12). Following our previous arguments we expect that such strengthening of the 3-electron bond will reduce the slope of descent of the D^+A^- curves (Figure 3), thereby raising the reaction barriers. Indeed, all these reactions have relatively high barriers despite the fact that in many of these cases the donor–acceptor ability of the reactants is more favorable than in the first set. Thus, the 3-electron bond strength emerges from Table II as an important factor governing reactivity. For example, if we compare the reactivities of CH_3O^- and CH_3S^- (runs 7,8) to those of Cl^- and Br^- (runs 2,3), we find that the donor–acceptor ability no longer controls reactivity. What makes the former two less reactive is their much stronger 3-electron bonds. It follows that *strengthening the 3-electron bond will result in sluggish reactivity even when the reactants simultaneously become a better donor–acceptor pair*. This reactivity pattern is what we termed earlier *3-electron bond controlled*, and it will be observed whenever the 3-electron bond strength varies greatly. The usefulness of this division is evident. For example, the barrier for CH_3S^- exchange (run 8) is smaller than that for HO^- exchange owing to the smaller $I_{X:} - A_{CH_3X}$ value and the same strengths of the 3-electron bonds. On the other hand, the similarity of the barriers for the reactions of HCC^- and NC^- arise from opposite trends in the two parameters. Another interesting comparison is between the reactions of $CF_3CO_2^-$ (run 5) and the reactions of HO^- and CH_3O^- (runs 6, 7). One can see that the relatively small barrier for $CF_3CO_2^-$ exchange originates in its very weak 3-electron bond.

These reactivity patterns can be expressed by rewriting eq 10 in a more explicit form:

$$E^* = r(I_{X:} - A_{CH_3X}) - |\beta| \qquad (23)$$

We can see that r will be determined by the 3-electron bond effect on the slope and will be common to all reactions within a family with roughly constant 3-electron bond strengths. Thus r determines the fraction of $I_{X:} - A_{CH_3X}$ which enters the activation barrier, and hence, it constitutes the sensitivity of the family to the donor–acceptor ability of the reactants.

We would now like to use eq 23 to analyze the gap–slope interplay in a semiquantitative manner. In order to obtain some idea about the value of r (eq 23), we have mimicked the two intersecting curves in our model (Figure 1b) by two parabolas.

(39) This trend was also noted by Lewis: Lewis, E. S.; Kukes, S.; Slater, C. D. *J. Am. Chem. Soc.* **1980**, *102*, 303–306, 1619–1623.

(40) The gas-phase barriers were calculated from the gas-phase data in ref 1. All the results were calibrated with respect to the barrier of the reaction: $CH_3O^- + CH_3Cl \rightarrow CH_3OCH_3 + Cl^-$,[1g] using the relation $\ln (k_1/k_2) = E_2^* - E_1^*$. The resulting barriers were used in the Marcus equation: $E^* = (\Delta H)^2/(16\Delta H_0^*) + \Delta H_0^* + {}^1/_2\Delta H$ (All ΔG's were replaced by ΔH. ΔH_0^* is the reaction's intrinsic barrier) as was done by Pellerite and Brauman.[1g] The results of ΔH_0^* were found much more sensitive to the values of ΔH than to those of E^*. We have then followed the recipe of Albery and Kreevoy,[3a] and we have calculated the barrier of each identity exchange reaction using ΔH_0^* values calculated from as wide a variety of reactions as possible. The values in Table II constitute the mean results.

Table III. Calculated Barriers (kcal/mol)[a] for Identity Reactions $X^-: + CH_3X \rightarrow XCH_3 + :X^-$

	set I			set II		
	X	E^* (r = 0.25)		X	E^* (r = 0.25)	E^* (r = 0.4)
(1)	F	19.5	(1)	HO	13.3	29.6
(2)	Cl	14.3	(2)	CH_3O	9.5	23.6
(3)	Br	10.8	(3)	CH_3S	8.8	22.4
(4)	I	6.3	(4)	HCC	20.3	40.8
(5)	CF_3CO_2	15.8	(5)	H	14.0	30.8 (48.7)[b]

[a] Using eq 23. The same $I_{X:} - A_{CH_3X}$ values as in Table II are used. $|\beta|$ = 14 kcal/mol throughout. [b] Using r = 0.56 in eq 23.

Using a dimensionless Q to symbolize the reaction coordinate, the energy expressions for the two curves become[41a]

$$E_1 = AQ^2 \tag{24}$$

$$E_2 = AQ^2 - kQ + (I_{X:} - A_{CH_3X}) \tag{25}$$

Thus, at Q = 0 the lower curve (E_1) has a minimum which corresponds to the encounter complex, and the two curves are separated by $I_{X:} - A_{CH_3X}$ which mimics $(DA)_r$ and $(D^+A^-)_r$ at the reaction starting point of Figure 1b.[24] The upper curve E_2 contains a stabilizing term ($-kQ$) which mimics the 2-electron bond making and the 3-electron relaxation effects of $(D^+A^-)_r$. At the product end, $Q = 2(I_{X:} - A_{CH_3X})/k$, the ordering of the two curves reverses, E_2 being below E_1 by $I_{X:} - A_{CH_3X}$, and this mimics the state correlation idea inherent in Figure 1b. Using this approach the barrier height is found to be of a form identical with eq 23 [and (10)] with a value of r = 0.25. If we incorporate the avoided crossing constant β we obtain

$$E^* = 0.25(I_{X:} - A_{CH_3X}) - |\beta| \tag{26}$$

Note that the value of r = 0.25 is that obtained from the Marcus theory of electron transfer.[37] Using other curve types we get analogous expressions with varying r depending on the steepness of the corresponding curves.[42,6a,f]

In order to see whether we can estimate S_N2 barriers in a semiquantitative fashion, we have applied eq 26 for those systems exhibiting weak 3-electron bonds. In order to reproduce a barrier of ~19 kcal/mol for the exchange reaction of F^-, a value of $|\beta|$ = 14 kcal/mol is required. Using this value of $|\beta|$, we have calculated the barriers for the rest of the group members (runs 1–5 in Table II). The results are listed in Table III as set I and show reasonable agreement with the gas-phase data in Table II.

We have also calculated barriers for those identity reactions with strong 3-electron bonds. As one can see from set II in Table III, when we use the slope parameter r = 0.25, the resulting barriers are far too low in comparison with experimental and computed results. A reasonable agreement is obtained only when we use a higher slope parameter r = 0.4 which adequately takes into account the strength of the 3-electron bonds in this group. This ratio of the slope parameters in the two sets closely resembles the ratio of their 3-electron bond strength parameter (a_2^2) from Tables I and II, and this relation can seve as a general recipe for selecting r values in eq 23. So in general we can see that the concept of gap–slope interplay reproduces the main reactivity trends of the identity reaction ensemble quite well, even at this naive level of application.

There is one result in Table III which still requires explanation. The calculated barrier for H^- is still too low in comparison with the gas-phase data of Table II (run 11), and a much higher slope parameter r = 0.56 is necessary if one wishes to reproduce the barrier. This suggests that the descent of the D^+A^- curves for this reaction involves yet another retarding effect which is not taken into accout in the 3-electron bond parameter.

The substrate CH_3–H contains four identical leaving groups. Hence the 3-electron bond in $(CH_4–H)^-$ is actually delocalized across the four linkages as shown schematically in eq 27:[43]

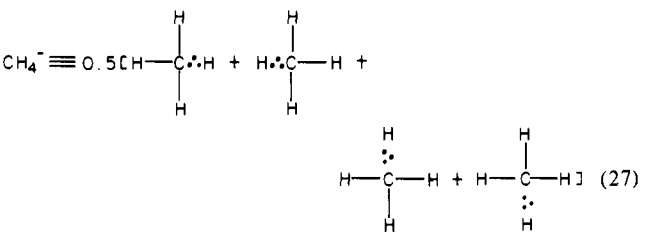

(27)

Each linkage has now 75% of the character of a full bond and only 25% of the character of a 3-electron bond. Thus, stretching such a linkage is energetically costly, and at the same time, since the extra electron is delocalized it also retards the new H–C bond making with the nucleophile. This localization requirement leads to a reduction in the D^+A^- slope of descent, and as a result a higher fraction of $I_{H:} - A_{CH_3-H}$ enters the activation energy (2nd reactivity rule in section II). We expect this extra localization to be important for substrates such as CH_2Cl_2, CCl_4, etc., and may well be the factor responsible for their low susceptibility to nucleophilic substitution in comparison with CH_3Cl.[44]

A similar extra localization requirement exists for delocalized nucleophiles like $CF_3CO_2^-$, NC^-, etc. Their delocalization causes a reduction in the D^+A^- slope of descent (2nd reactivity rule). Consider, for example, the $CF_3CO_2^-$, CH_3–$OCOCF_3$ reactant pair. Within D^+A^- the $CF_3CO_2\cdot$ species is delocalized through the following resonance interaction:

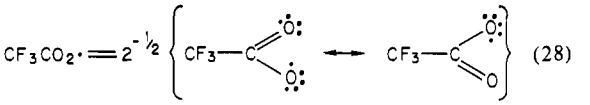

(28)

During the descent of D^+A^-, $CF_3CO_2\cdot$ interacts with $\cdot CH_3$ to form CF_3COO–CH_3, and *therefore it must localize to only one of the forms in eq 28 so that the new O–C bond may be generated.* Or, put differently, the energetic advantage gained by the resonance stabilization of $CF_3CO_2\cdot$ must be lost again on formation of the O–C bond.[45] As long as the localization of $CF_3CO_2\cdot$ has not yet been effected, the new O–C bond with the substrate cannot be fully realized. Therefore, the delocalization of the nucleophile effectively retards the new bond formation and slows down the D^+A^- slope of descent. *It follows that in the reactions where*

(41) (a) The parabolic description of the curves can be understood in terms of expanding the reaction Hamiltonia and retaining up to the quadratic terms in the reaction coordinate (Q). $\hat{H}(Q_0) + (\partial\hat{H}/\partial Q)_{Q_0}Q + {}^1/_2(\partial^2\hat{H}/\partial Q^2)_{Q_0}Q^2 + \ldots$. Then $A = {}^1/_2\langle\psi_i|(\partial^2\hat{H}/\partial Q^2)_{Q_0}|\psi_i\rangle$ were ψ_i is either $(DA)_r$ or $(D^+A^-)_r$. K arises from the linear term, i.e., $k = -\langle(D^+A^-)_r|(\partial\hat{H}/\partial Q)_{Q_0}|(D^+A^-)_r\rangle = -[\partial E[(D^+A^-)_r]/\partial Q]_{Q_0}$ and can be given an interpretation as the relaxation of $(D^+A^-)_r$ owing to 3-electron bond reorganization and 2-electron bond making. The same results are obtained if one uses two separate coordinates: one, Q_1, describing the approach of X^- to CH_3X and the other, Q_2, the C–X stretching in CH_3X. For a similar approach to curve crossing (for problems of vibronic coupling), see, for example, Köppel, H.; Domcke, W.; Cederbaum, L. S.; von Niessen, W. *J. Chem. Phys.* **1978**, *69*, 4252. (b) The positions of the encounter complexes are set at $Q_r = Q_0 = 0$ and at $Q_p = 2(I_{X:} - A_{CH_3X})/k$ (obtained from $\partial E_2/\partial Q = 0$ in eq 25). For the nonidentity exchange one uses the relation $E_1(Q_r) - E_2(Q_p) = \Delta H$ where Q_r and Q_p have the above expressions (however, use $I_{N:}$ instead of $I_{X:}$).

(42) The underlying idea here is that one can use different curve types to describe the reaction potential curve. For an excellent review, see: Agmon, A. *Int. J. Chem. Kinet.* **1981**, *13*, 333–365.

(43) In VB terms this would require at least 8 determinants if at each structure the three 2-electron bonds will be treated as a core of doubly occupied bond MOs. In molecular orbital terms one can approximate our CH_4^- valence state and use CH_4 with an extra electron in the delocalized LUMO of CH_4.

(44) See, for example: Hine, J.; Stanton, J. E.; Brader, W. H., Jr. *J. Am. Chem. Soc.* **1956**, *78*, 2282–2284. Hine, J.; Thomas, C. H.; Stanton, J. E. *Ibid.* **1955**, *77*, 3886–3889.

(45) It must be remembered (eq 11) that our $I_{X:}$ value for $CF_3CO_2^-$ reflects the energy needed to ionize the anion leaving behind a delocalized $CF_3CO_2\cdot$ (eq 28). We could, of course, artifically build our $(D^+A^-)_r$ anchor point using a localized (ready for bonding) $CF_3CO_2\cdot$. In such a case the $I_{X:}$ value would be higher by the resonance energy of $CF_3CO_2\cdot$, and the special localization effect would have entered into the energy gap. The same considerations apply to the case of CH_4^-, where we could have started with one localized form (eq 27) in whiih the electron resides in the linkage to be cleaved along the reaction coordinate.

X^-:($X\cdot$) is a delocalized species one must use a higher slope parameter, r, than the one suggested by soley considering the $(C\therefore X)^-$ bond strength. This could be the reason why in order to reproduce the barrier for exchange of $CF_3CO_2^-$ we need to use $r = 0.25$–0.27, although the extreme weakness of its 3-electron bond would have suggested that $r \sim 0.15$ be a more adequate value. The same considerations apply to the reaction of $NC:^-$ and thus the poor NC^-:/CH_3–CN reactivity is seen originating in the poor acceptor ability of CH_3–CN (strong C–CN bond) as well as the low nucleophilicity of NC^-: brought about by the delocalized nature of NC^-: [i.e., ($:N\equiv C\cdot$) ↔ $\lambda(\cdot N\equiv C:)$].[45]

We conclude therefore that whenever the 3-electron bonds are weak (localized), one can use $r \leq 0.25$, whereas for strong (delocalized) 3-electron bonds and when special localization requirements occur, one must use $r \geq 0.25k$. The value of k is larger than 1 and may be approximated by the ratio of the 3-electron bond strength parameters (a_2^2 in Table I) of the reaction in question to that in a standard reaction with a weak 3-electron bond. Using this information, we can briefly consider reactivity trends in exothermic reactions.

V. The Role of Reaction Exothermicity

From the thermochemical relationship in eq 12 it becomes evident that ΔH is linked with all the other reactivity factors. Therefore as we change from an identity reaction $X^-: + CH_3X \rightarrow X\text{–}CH_3 + :X^-$ to a nonidentity reaction $N^-: + CH_3X \rightarrow N\text{–}CH_3 + :X^-$, the change in ΔH may involve a change in the 2-electron bond strengths (N–C vs. X–C), a change in the energy gap ($I_{N:} - A_{CH_3X}$ vs. $I_{X:} - A_{CH_3X}$), and a change in strengths of the 3-electron bond with the nucleophile (N∴C vs. X∴C). Each such change is likely to manifest itself in the relative reactivity of the two reaction systems. Therefore, the effect of reaction exothermicity on the reaction barrier is not as simple as might be expected from a *straightforward* application of the Bell–Evans–Polanyi (BEP) principle.[8]

In order to anticipate the various possibilities, we need to derive an expression, analogous to the one in eq 23, but which incorporates ΔH. Therefore we have mimicked the curve intersection (Figure 1b) by two parabolas whose minima differ by ΔH[41b] which is taken to be the energy difference between the encounter complexes (N^-:(CH_3–X) and (N–CH_3):X^-).[26] The expression for the barrier reads

$$E^* = 0.25(I_{N:} - A_{CH_3X})^2/[(I_{N:} - A_{CH_3X}) - \Delta H] - |\beta| \qquad (29)$$

Using a common expression,[1e] $\Delta H = A_{N\cdot} - A_{X\cdot} + H^0_{C\text{-}X} - H^0_{N\text{-}C}$ (recall $I_{N:} = A_{N\cdot}$, etc.) and substituting into eq 29, one obtains

$$E^* = 0.25(I_{N:} - A_{CH_3X})^2/(I_{X:} - A_{CH_3X} + H^0_{N\text{-}C} - H^0_{C\text{-}X}) - |\beta| \qquad (30)$$

Let us consider first a case where a change in ΔH is expressed mainly as a change in the 2-electron bond strength while the gap factor ($I_{N:} - A_{CH_3X}$) and the 3-electron bond strengths remain constant. Such an example is shown below:

$$Cl^- + CH_3\text{–}Cl \rightarrow Cl\text{–}CH_3 + Cl^- \qquad (31)$$

$$F^- + CH_3\text{–}Cl \rightarrow F\text{–}CH_3 + Cl^- \qquad (32)$$

Comparing the reactivity factors for the two reactions we find that the energy gaps are nearly equal; $I_{Cl:^-} - A_{CH_3Cl} = 113$ kcal/mol and $I_{F:} - A_{CH_3Cl} = 106$ kcal/mol (using $A_{CH_3Cl} = -30$ kcal/mol from Table I). This is also true of the strengths of the 3-electron bonds (C∴F)$^-$ and (C∴Cl)$^-$ ($a_2^2 = 0.22$ and 0.25, respectively in Table I). The only factor which changes markedly is the strength of the incipient 2-electron bonds; while $H^0_{C\text{-}F}$ is ~108 kcal/mol, $H^0_{C\text{-}Cl}$ is only ~83 kcal/mol. This bond strength difference will result in a steeper $(D^+A^-)_r$ descent for the exothermic reaction (eq 32), much like the case discussed in Figure 4, and will therefore lead to a smaller barrier. Indeed, if we use eq 30 [or (29)] to calculate barriers, we find ($|\beta| = 14$ kcal/mol; $A_{CH_3Cl} = -30$ kcal/mol) $E^* = 14.25$ kcal/mol for the identity reaction (eq 31), while for the exothermic reaction (eq 32) E* is only 6.5 kcal/mol. The latter is close to the values obtained by Pellerite and Brauman (5.8 – 8.1 kcal/mol).[1g] *Thus the superior gas-phase nucleophilicity of F^- (vs. Cl^-) is a slope effect which originates in its stronger C–F 2-electron bond* (see related discussion by Bohme in ref 1e).

Another example where the BEP principle applies is the comparison of the F^-/CH_3F and F^-/CH_3Cl reactant pairs. Here the incipient 2-electron bonds are the same, and the 3-electron bonds have approximately the same strengths. Therefore, the reaction exothermicity expresses itself in this case mainly through the $I_{N:} - A_{CH_3X}$ factor (see also eq 12). Equation 30 predicts that the better acceptor substrate, CH_3Cl, will react faster with F^- ($E^* = 6.5$ vs. 19.5 kcal/mol, see also Table III for F^-/CH_3F). *Thus whenever an increase in reaction exothermicity involves mainly a decrease in the $I_{N:} - A_{CH_3X}$ factor, the reaction barrier will decrease.*

Equation 30 still does not take into account that strong 3-electron bonds as well as other localization requirements (e.g., eqs 27 and 28) cause a larger fraction (than 0.25) of the gap ($I_{N:} - A_{CH_3X}$) to enter the activation barrier (Figure 3). Therefore we shall replace the 0.25 factor by a variable n like we did for the identity reactions. Now the equation reads

$$E^* = \left[\frac{n}{(I_{X:} - A_{CH_3X} + H^0_{N\text{-}C} - H^0_{C\text{-}X})}\right][(I_{N:} - A_{CH_3X})]^2 - |\beta| \qquad (33)$$

Following the rules given at the end of the previous section, n ~0.25 for weak 3-electron bonds, while $n > 0.25$ for cases with strong 3-electron bonds (e.g., C∴OH) and whenever special localization requirements are imposed (e.g., eq 27 and 28).

In principle, eq 33 predicts that large changes in n can counteract an increase in the reaction exothermicity and thereby lead to a breakdown of the BEP principle. In fact such cases have been observed by both Bohme[1e] and Brauman.[1f] For example, the nucleophilicity of Cl^- and NC^-: toward CH_3Br is about the same[1e,f] although the reaction of NC^- is much more exothermic, and the C–CN bond is far stronger than the C–Cl bond. The reason for this behavior is linked with the localization requirement associated with NC· which was discussed above. This requires a larger n value in eq 32 for the NC^-:/CH_3Br pair. Using $n = 0.3$ and $A_{CH_3Br} = -21$ kcal/mol (Table I), we obtain $E^* = 10.5$ kcal/mol for NC^-:/CH_3Br, while a value of $n = 0.25$ yields the same barrier for the Cl^-/CH_3Br pair ($|\beta| = 14$ kcal/mol). Similar explanations which account for the poor reactivity of delocalized nucleophiles like NC^- and $PhCH_2^-$ were given by Bohme[1a,e] and Brauman.[1f,g] *Thus in these cases the BEP principle breaks down due to localization requirements of the nucleophile.*

Another aspect of the role of ΔH arises from comparing the reactivities of the pairs, e.g., F^-/CH_3Cl vs. H^-/CH_3F. Here, the second pair is better donor–acceptor pair ($I_{H:} - A_{CH_3F} \simeq 77$ kcal/mol; $I_{F:} - A_{CH_3Cl} \simeq 106$ kcal/mol) and it also leads to a more exothermic reaction ($\Delta H = -32$ vs. -57 kcal/mol). Despite these facts the pair H^-/CH_3F reacts much slower than the pair F^-/CH_3Cl.[1e] Here too the deviation from the BEP principle is linked with the strength and the delocalized nature of the (H∴C)$^-$ bond (see eq 27) which requires a large n ($n \sim 0.56$) and hence causes a larger fraction of the initial gap ($I_{H:} - A_{CH_3F}$) to enter the activation barrier. Thus, *whenever the increase in reaction exothermicity brings about large changes in 3-electron bond strengths or induces special localization requirement, a decrease in the reaction barrier is not guaranteed.*

VI. Conclusions

We have asked at the outset what is the electronic origins of the barrier in the S_N2 reaction and what are the factors which determine its height? We may now conclude that the S_N2 barrier arises from an avoided crossing of two curves which contain the reactant-like and the product-like Heitler–London VB forms. The energy gaps between the curves are $I_{N:} - A_{CH_3X}$ and $I_{X:} - A_{CH_3N}$ at the two reaction ends. Between the four anchor points there obtains a barrier. *The height of this barrier for the forward*

reaction is a fraction of the energy gap at the reactant end, and it takes the general form $E^* = r(I_{N:} - A_{CH_3X}) - |\beta|$. r is a factor which depends on the slopes of descent and the type of the two intersecting curves. This equation can be applied to thermoneutral as well as to exothermic (and endothermic) reactions, and thus it compliments both the Marcus equation and the BEP principle.

The slopes of descent of the intersecting curves are influenced, amongst other factors, by (a) the amount of delocalization (strength) of the 3-electron bonds $(C\therefore X)^-$ and $(C\therefore N)^-$, (b) specific localization requirements, e.g., in CH_3–H (eq 27) or in $CF_3CO_2^-$, NC^- (eq 28), and (c) the C–X and N–C bond strength difference. As the 3-electron bonds become stronger and the localization requirement more severe, the descent of the curves is retarded and a larger fraction of the gap $(I_{N:} - A_{CH_3X})$ enters the activation barrier (r is large). On the other hand, as the 2-electron bond strength (N–C vs. C–X) differences increase, a smaller fraction of the gap enters the activation barrier.

Thus, in general the ensemble of S_N2 reaction will exhibit (a) *electron-transfer-controlled* reactivity patterns which obey the donor–acceptor (or gap $I_{N:} - A_{CH_3X}$) abilities of the reactants[29] and (b) *slope-controlled reactivity patterns which respond* to the strengths of the 3-electron bonds, localization effects, etc. An important conclusion is that improving the donor–acceptor abilities of the reactants does not guarantee high S_N2 reactivity if at the same time this improvement creates severe localization demands. An example is the sluggish S_N2 reactivitites of the good electron acceptors CCl_4 and CH_2Cl_2[44] in comparison with the poorer acceptor CH_3Cl. However, since the position of crossing ("late" vs. "early") depends on the donor–acceptor abilitites (the gap $I_{N:} - A_{RX}$),[4b,46] their significant improvement is likely to lead to bona fide electron-transfer reactions, especially if such an improvement also creates specific localization requirements (e.g., in CCl_4)[47] which now takes place after crossing occurs.

Strong 3-electron bonds and specific localization requirements are also the cause for the breakdown of the universality of the BEP principle. The BEP principle is shown to apply with certainty only when an increase in reaction exothermicity does not involve significant changes in these factors.

In the future we hope to consider the effect of solvent on the barrier height as well as the concepts of nucleophilicity and leavhing group ability using eq 32.

Acknowledgment. We are indebted to Dr. S. Efrima for helpful suggestions and Professor J. F. Bunnett for stimulating discussions. S.S.S. thanks Dr. H. Köppel for very enlightening discussions on curve crossing.

Registry No. F, 16984-48-8; Cl, 16887-00-6; Br, 24959-67-9; I, 20461-54-5; HO, 14280-30-9; CH_3O, 3315-60-4; CF_3CO_2, 14477-72-6; CH_3S, 17302-63-5; NC, 57-12-5; HCC, 29075-95-4; H, 12184-88-2; H_2N, 17655-31-1; CH_3F, 593-53-3; CH_3Cl, 74-87-3; CH_3Br, 74-83-9; CH_3I, 74-88-4; $CF_3CO_2CH_3$, 431-47-0; CH_3OH, 67-56-1; CH_3OCH_3, 115-10-6; CH_3SCH_3, 75-18-3; $N{\equiv}CCH_3$, 75-05-8; $HC{\equiv}CCH_3$, 74-99-7; CH_4, 74-82-8; H_2NCH_3, 74-89-5; CH_3F radical anion, 34475-43-9; CH_3Cl radical anion, 69685-01-4; CH_3Br radical anion, 40431-10-5; CH_3I radical anion, 40431-11-6; CH_3OH radical anion, 68474-04-4; CH_3OCH_3 radical anion, 81132-07-2; $CF_3CO_2CH_3$ radical anion, 81096-78-8; CH_3SCH_3 radical anion, 70332-64-8; $NCCH_3$ radical anion, 28486-62-6; $HC{\equiv}CCH_3$ radical anion, 81132-08-3; CH_4 radical anion, 27680-53-1; H_2NCH_3 radical anion, 81096-79-9.

(46) Using eq 25 and 24 it is possible to show that the position of the intersection point (Q_c) is $Q_c = (I_{N:} - A_{RX})/k$. This means that when $I_{N:} - A_{RX}$ approaches zero, the crossing point approaches the reactant (r) position, $Q_r = 0$.

(47) See, for example: (a) Meyers, C. Y.; Kolb, V. M. *J. Org. Chem.* **1978**, *43*, 1985–1990. (b) Ashby, E. C.; Goel, A. B.; Depriest, R. N. *J. Org. Chem.* **1981**, *46*, 2431–2433. (c) Ashby, E. C.; Goel, A. B.; DePriest, R. N. *J. Am. Chem. Soc.* **1980**, *102*, 7779. (d) Ashby, E. C.; Goel, A. B.; DePriest, R. N.; Prasad, H. S. *Ibid.* **1981**, *103*, 973. (e) Ashby, E. C.; DePriest, R. N.; Goel, A. N. *Tetrahedron Lett.* **1981**, *22*, 1763–1766.

Ab Initio Studies of the Structures of Peroxides and Peroxy Radicals

Raymond A. Bair[†] and William A. Goddard III*

Contribution No. 6508 from the Arthur Amos Noyes Laboratory of Chemical Physics, California Institute of Technology, Pasadena, California 91125. *Received August 14, 1981*

Abstract: Ab initio theoretical calculations of the equilibrium structures of CH_3OOCH_3, CH_3OOH, HOOH, $CH_3OO\cdot$, and $HOO\cdot$ are compared. The wave functions are calculated by using generalized valence bond (GVB) and configuration interaction methods. It is found that CH_3OOCH_3 is trans (planar), while CH_3OOH and HOOH exhibit dihedral angles of 126° and 119°, respectively. The theoretically determined structures of HOOH and $HOO\cdot$ agree closely with the accepted experimental structures. For the remaining species, very few experimental structural parameters are available.

Alkyl peroxides play an important part in hydrocarbon oxidation processes, yet few structural data are available, and reliable theoretical studies have previously been limited to the hydroperoxy species. In this study we have carried out ab initio generalized valence bond (GVB) and configuration interaction (CI) studies of the structures of the hydroperoxides, methyl peroxides, and the corresponding peroxy radicals:

$$HOOH,\ CH_3OOH,\ CH_3OOCH_3,\ HOO\cdot,\ CH_3OO\cdot$$

In all of these species it is necessary to include electron correlation in the wave function to determine an accurate equilibrium structure. Our calculations agree closely with the well-established experimental structures for HOOH and $HOO\cdot$, giving strong support to the reliability of calculated structures for the remaining species.

Table I. Equilibrium Structure of $CH_3O\cdot$

	r_{CO}	r_{CH_a}	r_{CH_s}	θ_{OCH_a}	θ_{OCH_s}
GVB + CI	1.410	1.112	1.111	111.1	106.9
exptl[a] (CH_3OCH_3)	1.410	1.100	1.091	110.8	107.2

[†]Chemistry Division, Argonne National Laboratory, Argonne, IL 60439

0002-7863/82/1504-2719$01.25/0